Archives of Toxicology (2018) 92:2275–2295
https://doi.org/10.1007/s00204-018-2226-8

ORGAN TOXICITY AND MECHANISMS

Aged rats are more vulnerable than adolescents to "ecstasy"-induced toxicity

R. Feio-Azevedo[1] · V. M. Costa[1] · D. J. Barbosa[1] · A. Teixeira-Gomes[1] · I. Pita[2] · S. Gomes[2] · F. C. Pereira[2] · M. Duarte-Araújo[3] · J. A. Duarte[4] · F. Marques[5] · E. Fernandes[6] · M. L. Bastos[1] · F. Carvalho[1] · J. P. Capela[1,7]

Received: 30 January 2018 / Accepted: 17 May 2018 / Published online: 4 June 2018

Abstract

3,4-Methylenedioxymethamphetamine (MDMA or "ecstasy") is a widespread drug of abuse with known neurotoxic properties. The present study aimed to evaluate the differential toxic effects of MDMA in adolescent and aged Wistar rats, using doses pharmacologically comparable to humans. Adolescent (post-natal day 40) (3×5 mg/kg, 2 h apart) and aged (mean 20 months old) (2×5 mg/kg, 2 h apart) rats received MDMA intraperitoneally. Animals were killed 7 days later, and the frontal cortex, hippocampus, striatum and cerebellum brain areas were dissected, and heart, liver and kidneys were collected. MDMA caused hyperthermia in both treated groups, but aged rats had a more dramatic temperature elevation. MDMA promoted serotonergic neurotoxicity only in the hippocampus of aged, but not in the adolescents' brain, and did not change the levels of dopamine or serotonin metabolite in the striatum of both groups. Differential responses according to age were also seen regarding brain p-Tau levels, a hallmark of a degenerative brain, since only aged animals had significant increases. MDMA evoked brain oxidative stress in the hippocampus and striatum of aged, and in the hippocampus, frontal cortex, and striatum brain areas of adolescents according to protein carbonylation, but only decreased GSH levels in the hippocampus of aged animals. The brain maturational stage seems crucial for MDMA-evoked serotonergic neurotoxicity. Aged animals were more susceptible to MDMA-induced tissue damage in the heart and kidneys, and both ages had an increase in liver fibrotic tissue content. In conclusion, age is a determinant factor for the toxic events promoted by "ecstasy". This work demonstrated special susceptibility of aged hippocampus to MDMA neurotoxicity, as well as impressive damage to the heart and kidney tissue following "ecstasy".

Keywords "Ecstasy" · Neurotoxicity · Aged rats · Tau · Cardiotoxicity · Nephrotoxicity

Abbreviations

5-HIAA	5-Hydroxyindoleacetic acid
5-HT	Serotonin

✉ R. Feio-Azevedo

✉ J. P. Capela
joaoc@ufp.edu.pt

1 UCIBIO, REQUIMTE (Rede de Química e Tecnologia), Laboratório de Toxicologia, Departamento de Ciências Biológicas, Faculdade de Farmácia, Universidade do Porto, Rua de Jorge Viterbo Ferreira, 228, 4050-313 Porto, Portugal

2 Instituto de Farmacologia e Terapêutica Experimental, Coimbra Institute for Clinical and Biomedical Research (iCBR), Faculty of Medicine, Universidade de Coimbra, Coimbra, Portugal

3 Departamento de Imunofisiologia e Farmacologia, Instituto de Ciências Biomédicas de Abel Salazar (ICBAS), Universidade do Porto, Porto, Portugal

4 CIAFEL, Faculdade de Desporto, Universidade do Porto, Porto, Portugal

5 UCIBIO, REQUIMTE, Laboratório de Bioquímica, Departamento de Ciências Biológicas, Faculdade de Farmácia, Universidade do Porto, Porto, Portugal

6 LAQV, REQUIMTE, Laboratório de Química Aplicada, Departamento de Química, Faculdade de Farmácia, Universidade do Porto, Porto, Portugal

7 FP-ENAS (Unidade de Investigação UFP em Energia, Ambiente e Saúde), CEBIMED (Centro de Estudos em Biomedicina), Faculdade de Ciências da Saúde, Universidade Fernando Pessoa, Porto, Portugal

ALT	Alanine aminotransferase
AST	Aspartate aminotransferase
ATP	Adenosine triphosphate
BSA	Bovine serum albumin
CHAPS	3-[(3-Cholamidopropyl)dimethylammonio]-1-propanesulfonate hydrate
CKMB	Creatine kinase MB isoenzyme
DA	Dopamine
DTT	Dithiothreitol
EDTA	Ethylenediamine tetraacetic acid
GFAP	Glial fibrillary acidic protein
GSH	Reduced glutathione
GSHt	Total glutathione
GSSG	Oxidized glutathione
HEPES	4-(2-Hydroxyethyl)piperazine-1-ethanesulfonic acid
5-HIAA	5-Hydroxyindoleacetic acid
HNE	Hydroxynonenal
HPLC	High-performance liquid chromatography
i.p.	Intraperitoneal
MDMA	3,4-Methylenedioxymethamphetamine (MDMA; "ecstasy")
NA	Noradrenaline
PBS	Phosphate-buffered saline
OD	Optic density
PMSF	Phenylmethanesulfonyl fluoride
PND	Post-natal day
p-Tau	Phosphorylated Tau
ROS	Reactive oxygen species
SERT	Serotonin transporter
SDS	Sodium dodecyl sulphate
TCA	Trichloroacetic acid
TPH	Tryptophan hydroxylase

Introduction

The ring-substituted amphetamine derivative 3,4-methylenedioxymethamphetamine (MDMA or "ecstasy") is a well-known and widely abused drug (Capela et al. 2009; Carvalho et al. 2012). The United Nations Office on Drugs and Crime estimated that 22 million people had used "ecstasy" in 2015 worldwide (UNODC 2017). According to the European Drug Report, 14 million European adults (aged 15–64) used MDMA at some time in their lives, and 2.3 million young adults (15–34) used MDMA in 2016 (EMCDDA 2017). Concerns on MDMA abuse especially rely on its serotoninergic neurotoxicity and on the long-term cognitive and psychiatric problems found in users (Capela et al. 2009; Carvalho et al. 2012; Klomp et al. 2012). In addition, toxic actions in the peripheral organs have been reported in humans, including cardiac, hepatic or renal toxicity (Andreu et al. 1998; Armenian et al. 2013).

In the rat's brain, MDMA induces acute noradrenaline (NA), serotonin [5-hydroxytryptamine (5-HT)] and dopamine (DA) release (Capela et al. 2009; Cuyas et al. 2014). As a long-term consequence of MDMA exposure, depletion of 5-HT and its metabolites, as well as decrease in 5-HT transport have been consistently reported in rats (Alves et al. 2009; Kindlundh-Hogberg et al. 2007; Reveron et al. 2005). In general, investigators wait 1 to 2 weeks following MDMA administration to confirm the long-lasting monoamine depletion evoked by the drug to laboratory animals (Broening et al. 1995; Capela et al. 2009; Goni-Allo et al. 2008a; Malberg and Seiden 1998). MDMA also inhibits the activity of tryptophan hydroxylase (TPH) and monoamine oxidase A (Capela et al. 2009; Che et al. 1995; Goni-Allo et al. 2008b). In addition, the increase of DA and 5-HT metabolism in the nerve endings and the MDMA metabolites contribute to the neurotoxic actions by increasing reactive oxidative species (ROS) formation (Alves et al. 2009; Capela et al. 2007; Colado et al. 1997).

Besides its central effects, MDMA also induces peripheral toxicity. In recreational users, MDMA promotes a sympathomimetic response with increased blood flow, increased heart rate and also hyperthermia, which in severe cases, can lead to rhabdomyolysis, kidney and liver failure, culminating in death (Hall and Henry 2006; Henry et al. 1992).

Hyperthermia has been consistently reported in laboratory animals after MDMA exposure, and it was shown to enhance MDMA neurotoxic actions (Che et al. 1995; Goni-Allo et al. 2008a). In addition, age seems to influence the hyperthermic response. In a study done by Broening and colleagues, young rats (PND10) exposed orally to MDMA (20 or 40 mg/kg) did not show any hyperthermic response, while rats at PND40 and PND70 showed an hyperthermic response after being exposed to the same dose of the drug (Broening et al. 1995). In a study conducted by Goni-Allo and colleagues, after administration of MDMA in a binge dose regimen [3 × 5 mg/kg, every 2 h, intraperitoneally (i.p.)], adult rats peaked temperatures above 39 °C (Goni-Allo et al. 2008a). Adolescent rats (PND 40), when exposed to the same dose regimen of the previous study, never surpassed 39 °C even after the third MDMA dose (Teixeira-Gomes et al. 2016). In agreement with these findings, there are some reports that argue for the importance of the age of exposure to MDMA either in humans (Klomp et al. 2012) or in rats (Kelly et al. 2002; Kolyaduke and Hughes 2013; Teixeira-Gomes et al. 2015). In rodents, MDMA neurotoxic effects seem to be less severe in perinatal, neonatal or even adolescent animals when compared to adult animals (Teixeira-Gomes et al. 2015). In humans, the age and the stage of brain development may influence the neurotoxic outcome after drug exposure. Human studies have shown that "ecstasy" consumed at early adolescence (first exposure 14–18 years old) and at late adolescence/young adult (first

exposure 18–36 years old) age have different outcomes on the 5-HT system projection densities, which was found to have an inverse relationship between groups (Klomp et al. 2012). Whereas in the adolescent group serotonin transporter (SERT) density was found to be elevated, in the adolescent/young adult group such hyperdensity was not observed. This finding was related to the brain maturation stage at the age of MDMA exposure (Klomp et al. 2012).

The adolescent brain is still in an active developing stage and the toxic effects to the brain and their later consequences are poorly known. The evaluation whether MDMA causes any type of effect on aging is still unknown. Furthermore, the consequences of MDMA misuse in the aged brain are undisclosed and studies in animals of different ages may render important findings, since the age factor contribution for MDMA toxic effects remains to be clarified.

The vast majority of studies do not explore the differential toxicity of MDMA to animals of dissimilar ages. Moreover, many reports conducted in laboratory animals frequently use high MDMA doses, rendering difficult the extrapolation to the human situation. Additionally, most studies focus on the neurotoxicity of MDMA and neglect the toxic events evoked by "ecstasy" to peripheral organs. Therefore, this work aimed to understand the differential toxic-related consequences of a moderate binge MDMA regimen to either adolescent or aged rats, with doses that are equivalent to those consumed by humans. Four brain areas (frontal cortex, striatum, hippocampus and cerebellum) and three peripheral organs (heart, liver and kidneys) were collected and studied regarding several biochemical and histological markers. To the best of our knowledge, this work was the first to expose aged animals to MDMA and compare the differential effects to adolescent animals, in such a broad panel of determinations.

Materials and methods

Materials

MDMA was extracted and purified from high purity MDMA tablets provided by the Portuguese Criminal Police Department, and transformed to the respective HCl salt. The MDMA salt was fully characterized by nuclear magnetic resonance and mass spectrometry (Capela et al. 2006, 2007). MDMA was dissolved in 0.9% NaCl and filtered using a 0.2-µM filter under a sterile environment.

Isoflurane (Isoflo® 100% p/p) was purchased from Abbot Animal Health, (Esteve Veterinaria, Italy). The local anaesthetic EMLA® (Lidocaine 25 mg/g + Prilocaine 25 mg/g) was purchased from AstraZeneca AB (London, UK).

The caspases 3 (Ac-Asp-Gln-Asp-MCA), 8 (Ac-Ile-Glu-Thr-Asp-MCA) and 9 (Ac-Leu-Glu-His-Asp-MCA) substrates were purchased from Peptanova (Sandhausen, Germany). The 4-(2-hydroxyethyl)piperazine-1-ethanesulfonic acid (HEPES), 3-[(3-cholamidopropyl) dimethylammonio]-1-propanesulfonate hydrate (CHAPS), dithiothreitol (DTT), Tris–HCl, reduced glutathione (GSH), oxidized glutathione (GSSG), nicotinamide adenine dinucleotide phosphate reduced form, Triton X-100, phenylmethylsulphonyl fluoride (PMSF), 5,5-dithio-bis(2-nitrobenzoic acid), glutathione reductase, bovine serum albumin (BSA), adenosine 5′-triphosphate disodium salt hydrate (ATP) (≥ 99% purity), and protease inhibitor cocktail were obtained from Sigma-Aldrich (St. Louis, MO, USA). ABX Pentra reagents were purchased from HORIBA (Kyoto, Japan).

The following primary antibodies were used: rabbit anti-dinitrophenyl primary antibody A-6430 from Thermo Fisher Scientific (MA, USA), rabbit polyclonal anti-phosphorylated protein Tau (p-Tau) at residue Ser396 SAB4504557, rabbit polyclonal anti-glial fibrillary acidic protein (GFAP) G9269, clone HM-2 M4403 and mouse monoclonal anti-α-tubulin antibody T6074 were all purchased from Sigma-Aldrich. The primary antibody rabbit polyclonal anti-4-hydroxynonenal (HNE) ab46545 was purchased from Abcam (Cambridge, United Kingdom). Anti-rabbit and anti-mouse IgG-peroxidase polyclonal antibodies and 0.45µm Amersham Protran nitrocellulose blotting membrane were purchased from Amersham Pharmacia Biotech (Buckinghamshine, United Kingdom). Bio-Rad RC DC protein assay kit, the Clarity™ Western ECL Substrate, Mini-PROTEAN® TGX™ Precast Gels and the nitrocellulose membranes (Trans-Blot® Turbo™ Mini Nitrocellulose Transfer Packs) were purchased from Bio-Rad Laboratories (Hercules, CA, USA). The bicinchoninic acid (BCA) protein assay was purchased from Thermo Fisher Scientific (MA, USA).

Histosec paraffin pastilles were obtained from Merck (Darmstardt, Germany). Xylene was purchased from Fischer Scientific (Loughborough, United Kingdom). Eosin 1% aqueous was purchased from Biostain (Traralgon, Australia). Harris Hematoxylin was purchased from Harris Surgipath (Richmond, IL, USA) and Histofluid from Marienfeld (Lauda-Königshofen, Germany). Other chemicals were obtained from Sigma-Aldrich, unless otherwise stated.

Animal model

Wistar male rats used in the study were bred in the rodent animal house facility of the Institute of Biomedical Sciences of Abel Salazar, University of Porto (ICBAS-UP). Housing and experimental treatment of the animals were in accordance with the guidelines defined by the European Council Directive (2010/63/EU) transposed into Portuguese law (Decreto-Lei no. 113/2013). Moreover, the experiments were performed with the approval of the Portuguese National Authority for Animal Health (General Directory of

Veterinary Medicine) (process no. 0421/000/000/2015) and the Ethical Committee of the Faculty of Pharmacy, University of Porto (process no. 17/03/2014). The animals were kept under controlled environment conditions (temperature 22.0 ± 2.0 °C, 40% humidity, 12 h light/dark cycles) and had *ad libitum* access to food and water. All procedures were carried out to provide appropriate animal care, minimizing their suffering and animals had permanent veterinary supervision throughout the experimental period.

Two groups of animals were used: ten adolescent rats at postnatal day (PND) 40 with an average weight of 165 g (protocol I) and 11 aged rats, with an average age of 20 months (18–22 months old) and average weight of 500 g (protocol II). We used PND40 rats as an adolescent model in accordance to our previous study (Teixeira-Gomes et al. 2016), and the 20 months old rats were considered a relatively 'early' stage of senescence (Slotkin et al. 2000). In fact, neurodegeneration, synaptic dysmorphology and peripheral organ dysfunction are likely to be present when very old animals are used, obscuring primary effects of lesion on synaptic or cellular function, and therefore we focused on early aged animals rather than examining animals at the later phase of life span (Slotkin et al. 2000). In addition, the expected mortality of very old animals could lead to the death of the animal during the handling due to natural causes.

Three days before the experiment, the dorsocervical region was trichotomised and a local anaesthetic (EMLA® Lidocaine 25 mg/g + Prilocaine 25 mg/g) was allowed to act for about 60 min. Then, each animal was subjected to a brief inhalatory anaesthesia with isoflurane, thus allowing the subcutaneous insertion of a temperature transponder (BioMedic Data Systems Inc., Seaford, DE) with minimum animal discomfort. This procedure ensures precise core body temperature measurements throughout the entire experimental period, as previously described by our group (Alves et al. 2009; Loureiro-Vieira et al. 2018; Teixeira-Gomes et al. 2016). Two different solutions of MDMA were prepared: 2.5 mg/mL (protocol I) and 5.0 mg/mL (protocol II) in sterile 0.9% saline solution as to assure that the administered volumes were within the recommended range for each animal age. For protocol I, on the day of the experiment, adolescent animals, which were housed in groups so that their conspecific social interactions could be maintained, were caged individually and divided into control ($n = 5$) or MDMA treated ($n = 5$) group. Three doses of sterile 0.9% saline solution were administered i.p. every 2 h to the control group, whereas three doses of 5 mg/kg of body weight of MDMA were administered i.p., every 2 h to the MDMA group ($MDMA_{total\ dose}$= 15 mg/kg of body weight). In each case, the injections were in different sides of the abdomen (left/right/left). Starting with the first dose of administration, the temperature of each animal was measured and registered every 15 min to a total of 6–7 h. To avoid any additional stress, the temperature was measured in the dorsal region of the animal without requiring any other manipulation. For the next 7 days, animals were monitored daily by specialized veterinarians. In addition, during this period the weight of the animal, food and water intake were recorded daily, as well as their temperature at approximately the same hour of the first injection. This MDMA binge dosing protocol (three doses of 5 mg/kg, i.p., every 2 h) used in adolescent rats was previously described in adult 10-week-old Wistar rats (mean 300 g body weight) to provide serotonergic toxicity (Goni-Allo et al. 2008a).

Protocol II used aged animals and the same procedure was done for the temperature transponder insertion. However, due to animal body size, no group housing was done before the day of MDMA administration to maintain animal comfort. On the day of the experiment, animals were divided into control ($n = 5$) or MDMA group ($n = 6$). In protocol II, two doses of MDMA 5 mg/kg of body weight were administered i.p., 2 h apart ($MDMA_{total\ dose}$ = 10 mg/kg of body weight), and controls received two saline injections. Of note, in this group one animal was eliminated from the study, because after the second dose, the body temperature surpassed 41.6 °C, and despite cooling measures, the animal remained lethargic and died after a few hours following MDMA administration. According to the allometric scaling principles, this 10 mg/kg dose is approximately equivalent to the dose of 15 mg/kg used in adolescent animals. Of note, the use of a dose regimen of three doses of 5 mg/kg in aged animals could lead to a high death rate.

Regarding the equivalence of these doses to humans, we calculated the equivalence to humans based on the allometric scaling principles using the formula human dose (mg/kg) = animal dose (mg/kg) × (animal weight/human weight)$^{1/4}$ (Beck et al. 2014). According to this relationship, the dose used in adolescent rats ($MDMA_{total\ dose}$ = 15 mg/kg of body weight) is approximately equivalent to 180 mg in a 50 kg human. Whereas the dose used in aged rats ($MDMA_{total\ dose}$ = 10 mg/kg of body weight) is equivalent to 200 mg in a 70 kg human. "Ecstasy" abusers normally take more than one tablet per session, ranging from two to four tablets in accordance with the binge-dosing pattern (Capela et al. 2009; Teixeira-Gomes et al. 2015). In Europe, the average content of MDMA in tablets has increased in recent years, and in accordance with the last European Union report on drugs of 2017, "ecstasy" tablets had an interquartile range of 50–110 mg with high purity (EMCDDA 2017). We estimate that the dose used in our protocol can be approximately equivalent to intake of two pills by humans using the binge-dosing pattern. Therefore, the present paradigm of MDMA exposure to animals mimics the dose schedule used by humans.

Tissue collection and treatment

On the 7th day after treatment, animals were anesthetized and euthanized in a chamber with isoflurane. Immediately following this procedure, blood was collected from the inferior vena cava and rats were immediately decapitated. Three organs were collected (heart, liver and kidneys) and four brain areas were dissected on ice (frontal cortex, hippocampus, striatum and cerebellum). Before sectioning, all four organs collected (brain, liver, heart and kidney) were weighted. These procedures were done in accordance with our previous reports (Loureiro-Vieira et al. 2018; Teixeira-Gomes et al. 2016).

Brain areas from the right side of the hemisphere were homogenized in RIPA buffer and treated as previously reported (Loureiro-Vieira et al. 2018; Teixeira-Gomes et al. 2016). The resulting supernatant was divided into two tubes: one for the quinoproteins assay and other for blotting analysis (slot blot and western blot assays), and were kept at − 80 °C until analysis. The left side of the hemisphere was collected into a perchloric acid solution 5% (w/v) and treated as we previously stated (Loureiro-Vieira et al. 2018; Teixeira-Gomes et al. 2016). The supernatant was separated for high-performance liquid chromatography (HPLC) analysis of biogenic amines, reduced glutathione/oxidized glutathione (GSH/GSSG) and ATP determination. Samples were maintained at − 80 °C until analysis. The pellet was also kept for protein determination and stored at − 20 °C.

Sections of $2mm^3$ from heart, kidneys and liver were collected into a 4% paraformaldehyde solution in a phosphate-buffered solution (PBS) and kept on ice for further histological treatment. Other pieces of these organs were also collected into a complete lysis buffer [25 mM HEPES, 5 mM $MgCl_2$, 1 mM ethylenediaminetetraacetic acid (EDTA), 0.5% Triton X-100 (v/v), 1 mM PMSF and 5 mM DTT, pH 7.4] for determination of caspases activity and immediately frozen at − 80 °C. Other fragments of the organs were stored in RIPA buffer (150 mM NaCl, 1% Triton X-100, 0.5% sodium deoxycholate, 0.1% sodium dodecyl sulphate, 50 mM Tris, 0.25 mM PMSF, 1 mM NaF, 1 mM $NaVO_3$ plus proteases inhibitor cocktail from Sigma-Aldrich, pH 8.0). At the day of the assay, all RIPA samples were homogenized using a sonicator (30 s, continuously), while maintaining the tube on ice to avoid excessive heating. The resulting homogenized product was centrifuged at 16,000*g*, 15 min at 4 °C, and the supernatant separated into tubes for the quinoproteins assay and slot-blot analysis, and immediately frozen at − 80 °C. The remaining organ portion was homogenized using an Ultra-Turrax homogenizer in a 0.1M KH_2PO_4 solution (pH 7.4) and several aliquots were collected. One aliquot of the homogenates was placed in perchloric acid at 5% (w/v) final concentration, and then centrifuged at 16,000*g*, for 10 min at 4 °C, and the resulting supernatant was collected and separated into tubes. They were immediately stored at − 20 °C for total GSH, GSSG or at − 80 °C for ATP determination. An aliquot of the initial organ homogenate was kept at − 20 °C for protein determination.

Measurement of plasma markers of hepatic or cardiac damage

The blood was collected in EDTA-containing tubes and centrifuged at 920*g* for 10 min, to separate the plasma. The plasma was frozen at − 20 °C until measurement of total creatine kinase (CK-R), creatine kinase MB isoenzyme (CKMB), aspartate aminotransferase (AST) and alanine aminotransferase (ALT) activities. These parameters were determined using enzymatic assays in the apparatus ABX Pentra 400 (HORIBA, Kyoto, Japan), as we previously reported (Loureiro-Vieira et al. 2018).

Histology procedures and optical microscopy analysis of tissue sections

All histological procedures were conducted according to previously published procedures (Dores-Sousa et al. 2015; Loureiro-Vieira et al. 2018; Teixeira-Gomes et al. 2016). The sections of heart, kidney and liver were subjected to two types of staining: hematoxylin and eosin for routine histological evaluation and Sirius red for fibrous tissue staining.

All preparations were analyzed and photographed using a Carl Zeiss Imager A1 light microscope equipped with AxioCam MRc 5 digital camera (Oberkochen, Germany). For Sirius red analysis, several sections from the heart, kidneys and liver of three animals from each group were done. Each animal/organ yielded one slide containing five tissue sections, which were photographed and analyzed using the Image-Pro Plus 6.0 software (Media Cybernetics, Inc., Rockville, MD, USA). The fibrous tissue stains bright red and the surrounding tissue stains yellow, which allows for a quantification of the percentage area of collagen (red) and surrounding tissues (yellow). The results are presented as percentage area *per* ratio of collagen/cardiomyocytes (heart), renal cells (kidney) or hepatic cells (liver), as previously reported by our group (Dores-Sousa et al. 2015).

Assessment of caspases 3, 8 and 9 activities

The activity of each caspase was assessed by fluorescence assays in peripheral organs, as previously described by our group (Dores-Sousa et al. 2015; Teixeira-Gomes et al. 2016). Briefly, after thawing, tissues were lysed in complete caspase assay lysis buffer and homogenized using a Potter AGV-8 Bunsen (Madrid, Spain). The samples were then centrifuged at 16,000*g*, 30 min at 4 °C, and the cytoplasmic fraction collected into new tubes that were kept on

ice. For the enzymatic reactions, 50 µL of cell lysates were placed in a black 96-well plate followed by 200 µL of assay buffer (100 mM NaCl, 50 mM HEPES, 1 mM EDTA, 10% glycerol (v/v), 0.1% CHAPS (w/v), 10 mM DTT, pH 7.4). The following substrates were used in a final concentration of 100 µM: Ac-Ile-Glu-Thr-Asp-MCA for caspase 8 activity, Ac-Leu-Glu-His-Asp-MCA for caspase 9 activity, and Ac-Asp-Gln-Asp-MCA for caspase 3 activity. As negative control, assay buffer (no cytoplasmic fraction) was used. The reaction mixture was incubated at 37 °C, for 24 h, after which fluorescence was evaluated (excitation 360 nm/emission 460 nm) using a microplate reader Biotech Synergy HT (Winooski, VT, USA). Results were normalized to the amount of protein sample loaded in each well. Caspase activity was expressed in fluorescent units per µg of protein (FU/µg protein).

Monoamines quantification by high performance liquid chromatography

The left brain areas were used for the determination of monoamine [DA, 5-HT and 5-hydroxyindoleacetic acid (5-HIAA)] contents by high-performance liquid chromatography with coulometric electrochemical detection (HPLC-CED), as previously described (Pereira et al. 2011). The acidic supernatants obtained were filtered (9,000*g*, 10 min, 4 °C) using 0.2-µm Nylon microfilters (Spin-X® Centrifuge Tube Filter). Monoamines were separated on a Grace Platinum EPS C18 column (4.6 mm × 150 mm; 100 Å; 5 µm) with a mobile phase (pH 2.5) consisting of potassium dihydrogen phosphate (25 mM), 1-heptane sulphonic acid (0.4 mM), EDTA (50 µM), 3% acetonitrile (v/v). Samples were quantified by an analytical cell (model 5011, ESA Analytical, Dorton Aylesbury, Buckinghamshire, UK) coupled to a Coulochem-II electrochemical detector (ESA, Analytical) and set at E1 = + 250 mV. Serotonin detection was achieved using a flow rate of 1 mL/min and a sensitivity of 100nA, while DA detection was achieved using a flow rate of 0.5 mL/min and a sensitivity of 500nA. Monoamine concentration in each sample was determined by comparison to peak areas of standards, and expressed in ng/mg protein.

Adenosine 5′-triphosphate levels

ATP levels in the heart, kidneys, liver and brain areas were assessed by a bioluminescent assay based on the firefly reaction of luciferin-luciferase system, as previously described (Costa et al. 2007). For each measurement, an ATP standard curve was done (ATP ≥ 99% purity according to Sigma-Aldrich). ATP in the samples/standards is consumed in the reaction of luciferin oxidation by the luciferase enzyme and emits light that is detected. Bioluminescence was immediately read in a microplate reader Biotech Synergy HT (Winooski, VT, USA). The results were expressed in nmol of ATP per mg of protein.

Total glutathione and oxidized glutathione levels

The determination of total glutathione (total GSH) and GSSG levels was done by the 5,5′-dithiobis(2-nitrobenzoic acid) (DTNB)-GSSG reductase recycling assay according to previous works (Costa et al. 2007; Teixeira-Gomes et al. 2016). The levels of GSH were determined considering the following ratio: GSH = total GSH − 2×GSSG. The results were expressed in nmol of GSH or GSSG per mg of protein.

Quinoprotein levels

To determine the protein-bound quinones (quinoproteins) in the different brain areas and also in peripheral organs, the nitrotetrazolium blue/glycinate assay was performed as detailed previously (Capela et al. 2007). RIPA lysates containing 50 µg of protein in the case of brain areas, and 25 µg of protein for the peripheral organs were used as samples, and the results were expressed in OD at 535 nm per mg of protein.

Protein carbonylation evaluation by slot blot

Protein carbonyls, an index of protein oxidation, were determined as previously described (Barbosa et al. 2012, 2015; Teixeira-Gomes et al. 2016). Samples were allowed to react with 2,4-dinitrophenylhydrazine, and then (0.2 µg) were loaded into nitrocellulose membranes under vacuum, using a Hybri-Slot apparatus (Filtration manifold, Gibco BRL, Life Technologies, Gaithersburg, MD, USA). Then, after washing and blocking, membranes were incubated with a rabbit polyclonal anti-dinitrophenylhydrazine primary antibody (1:1,000) overnight, at 4 °C. After washing, membranes were then incubated with the anti-rabbit IgG-peroxidase secondary antibody (1:2,000) for 2 h, at room temperature. Immunoreactive bands were detected using the Clarity™ Western ECL Substrate, according to the supplier's instructions. Digital images were acquired using a Molecular Imager® ChemiDoc™ XRS + System (Bio-Rad Laboratories, CA, USA) and analyzed with Image Lab™ Software (Bio-Rad Laboratories, CA, USA). Optical density results were expressed as % of control values.

Western blot analysis

Samples were diluted to an equal protein concentration, and 50 µL were mixed with 50 µL SDS-PAGE reducing buffer [4% SDS(w/v), 125 mM Tris base (pH 6.8), 15% glycerol (v/v), 1% bromophenol blue (w/v), and 20% β-mercaptoethanol (v/v)]. 60 µg of protein were loaded and

separated in Mini-PROTEAN® TGX™ Precast Gels, at a constant voltage of 150 mV, using a running buffer [25 mM Tris Base, 19 mM glycine, and 0.1% SDS (w/v), pH 8.6]. Gels were transferred to nitrocellulose membranes (Trans-Blot® Turbo™ Mini Nitrocellulose Transfer Packs), at a constant amperage of 2.5 mA, for 10 min, in a Trans-Blot® Turbo™ Transfer System (Bio-Rad Laboratories). Membranes were then rinsed in TBS-T, and non-specific sites were blocked for 1 h, at room temperature, in blocking buffer [5% milk (w/v) in TBS-T]. Membranes were incubated with primary antibodies overnight at 4 °C: rabbit polyclonal anti-phospho-Tau Ser396 (1:5,000), and rabbit polyclonal anti-GFAP (1:500). After washing five times (10 min each) with TBS-T, membranes were then incubated with the anti-rabbit IgG-peroxidase (1:2,000 or 1:1,000, respectively) secondary antibody, for 2 h, at room temperature. All antibodies were diluted in blocking buffer. For protein loading control, membranes were routinely stripped in stripping buffer [0.7% β-mercaptoethanol (v/v) in 63 mM Tris–HCl, pH 6.8, and 2% SDS (w/v)] for 30 min, at 65 °C, blocked for 1 h, at room temperature, in blocking buffer, and reprobed with mouse monoclonal anti-α-tubulin antibody (1:5,000), overnight, at 4 °C. This was followed by the anti-mouse IgG-peroxidase (1:2,000) secondary antibody incubation, for 2 h, at room temperature. Following three washes (10 min each) with TBS-T, immunoreactive bands were detected using the Clarity™ Western ECL Substrate, according to the supplier's instructions. Digital images were acquired using a Molecular Imager® ChemiDoc™ XRS + System (Bio-Rad Laboratories, CA, USA) and analyzed with Image Lab™ Software (Bio-Rad Laboratories, CA, USA). To normalize phospho-Tau Ser396 and GFAP immunoreactivity, the OD ratios of these proteins to the loading control of α-tubulin were calculated. Results were presented as OD ratio of the protein of interest/α-tubulin.

Assessment of 4-hydroxynonenal immunoreactivity by slot blot

Immunocontent of 4-HNE-modified proteins was determined as previously described (Yin et al. 2009), with adaptations. 30 µg of protein were loaded into nitrocellulose membranes under vacuum, using a hybrid-slot filtration manifold apparatus (Gibco BRL, Life Technologies Gaithersburg, MD, USA). Then, after washing with TBS-T, non-specific sites were blocked for 1 h, at room temperature, in blocking buffer [5% milk (w/v) in TBS-T]. Membranes were then incubated with rabbit polyclonal anti-4-HNE primary antibody (1:1,000) overnight, at 4 °C. After washing five times (10 min each) with TBS-T, membranes were then incubated with the anti-rabbit IgG-peroxidase secondary antibody (1:1,000) for 2 h, at room temperature. Antibodies were diluted in blocking buffer. Following three washes (10 min each) with TBS-T, immunoreactive bands were detected using the Clarity™ Western ECL Substrate, according to the supplier's instructions. Digital images were acquired using a Molecular Imager® ChemiDoc™ XRS + System (Bio-Rad Laboratories, CA, USA) and analyzed with Image Lab™ Software (Bio-Rad Laboratories, CA, USA). Optical density results were expressed as % of control values.

Protein quantification

The quantification of the protein content on tissue homogenates or brain's protein pellet was done according to the standard Lowry method or the bicinchoninic acid (BCA) protein assay. For samples containing high concentrations of detergents or reducing agents (RIPA buffer or caspase lyses buffer), the DC™ Protein Assay kit (Bio-Rad Laboratories, CA, USA) was used according to the manufacturer's instructions. Standard curves were done using BSA protein.

Statistical analysis

Results are presented as mean ± standard deviation (SD). Statistical analysis was conducted using GraphPad Prism version 6 (GraphPad Software, CA, USA). Outliers were identified by the ROUT test ($Q = 1\%$) and removed before further statistical analyses. The Shapiro–Wilk normality test was conducted before group comparison. When two groups were compared, the unpaired *t* test was used for data that followed a normal distribution or the Mann–Whitney rank sum test, if data did not pass the normality test. Regarding the statistical analysis of temperature, animal weight, food and water intake, a two-way analysis of variance (ANOVA), with repeated measurements, was used followed by Bonferroni post hoc test, once a significant p was achieved. Statistical significance was accepted at p values lower than 0.05.

Results

The MDMA-induced hyperthermic response in aged rats was more marked than in adolescent animals

MDMA administration to laboratory animals is known to evoke an hyperthermic response (Capela et al. 2009; Teixeira-Gomes et al. 2015), and binge doses were shown to promote hyperthermia in rats (Goni-Allo et al. 2008a; Teixeira-Gomes et al. 2016). Herein, aged rats attained higher levels of body temperature when compared to adolescent animals (Fig. 1). Both adolescent and aged animals revealed a hyperthermic response following MDMA doses that are equivalent to the human use. Adolescent rats already showed a temperature increase after the first dose of 5 mg/kg of MDMA at 105 min when compared

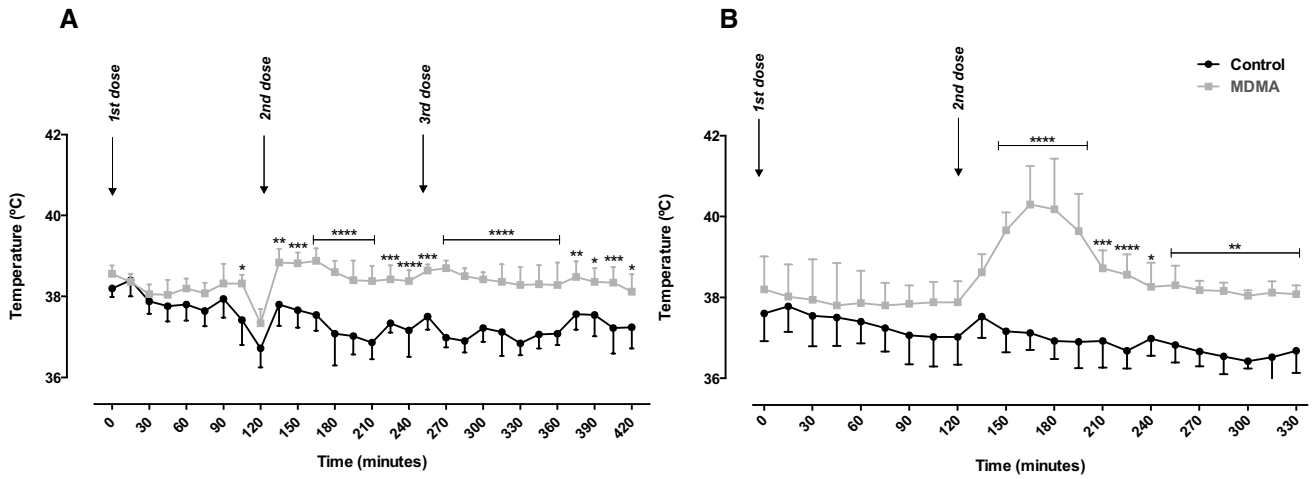

Fig. 1 Temperature (°C) of control and MDMA exposed animals in adolescent (**A**) and aged (**B**) groups. Temperature was monitored following the first dose throughout 420 min for the adolescent [control $n=5$; MDMA $n=5$] and for 330 min in the case of aged [control $n=5$; MDMA $n=5$] animals (*$p<0.05$, **$p<0.01$, ***$p<0.001$ and ****$p<0.0001$ MDMA versus control at the same timepoint)

to the control group (Fig. 1A). After the second and third MDMA administrations, the temperature of the MDMA group remained elevated and significantly different from the control group up to 420 min (Fig. 1A). The highest mean temperature presented by the adolescent MDMA-treated animals was 38.8 °C and it was reached at 165 min. The difference of temperature between MDMA-treated and control adolescent animals ranged from 1 to 1.5 °C, even following three doses of 5 mg/kg leading to a cumulative dose of 15 mg/kg. In the case of aged rats, after the first MDMA dose of 5 mg/kg no significant temperature differences were found to controls (Fig. 1B). However, after the second dose of MDMA, which was given 2 h after the first administration, the temperature of the MDMA group increased and remained significantly elevated in comparison to controls until 330 min. The temperature reached in some animals a maximum of 41 °C at 165 min, and around this timepoint the differences towards control animals attained a mean of 3 °C (Fig. 1B).

Animals' temperature was assessed daily during the next 7 days after MDMA administration, to ascertain whether MDMA could promote thermoregulation impairment. Interestingly, on the first day post-MDMA exposure, MDMA-treated aged animals showed higher temperature when comparing to controls, attaining more than one degree of difference (Fig. 2A2). These body temperature differences between aged treated and controls were abolished in the next 6 days. Meanwhile, MDMA-treated adolescent animals did not present any difference to controls in the temperature during the days following MDMA exposure (Fig. 2A1). Once again, aged animals are more prone to the MDMA-evoked effects in body temperature than adolescents, revealing thermoregulatory impairment 24 h following MDMA exposure.

Regarding the animal behavior observed following MDMA exposure, adolescent-treated animals revealed signs of greater motor activity and piloerection than controls. In the case of aged animals, in the first minutes following the second MDMA dose there were signs of greater motor activity, then followed by signs of decreased motor activity, with prostration, increased salivary secretion, exophthalmos and discomfort.

MDMA treatment led to changes in food and water intake only in the aged group

The body weight, food and water intake of animals were monitored daily during 7 days, until the day of sacrifice. Regarding the adolescent group, only on the first day post-exposure a significant decrease on the body weight of the MDMA group was observed (Fig. 2B1). However, no differences were found regarding food and water consumption among groups on the days following MDMA exposure (Fig. 2C1, D1).

When considering the aged group, there was a significant difference between the control and the drug-exposed animals during the 2 days post-administration regarding food intake. A significant decrease on the food intake for the MDMA group on the first day was followed by a significant increase on the second day post-treatment (Fig. 2C2). Of note, there was a significant increase in water consumption in MDMA-treated aged rats on the first and second days post-MDMA administration (Fig. 2D2). Meanwhile, no differences were found among control and MDMA-treated aged animals in terms of body weight throughout the 7 days (Fig. 2B2).

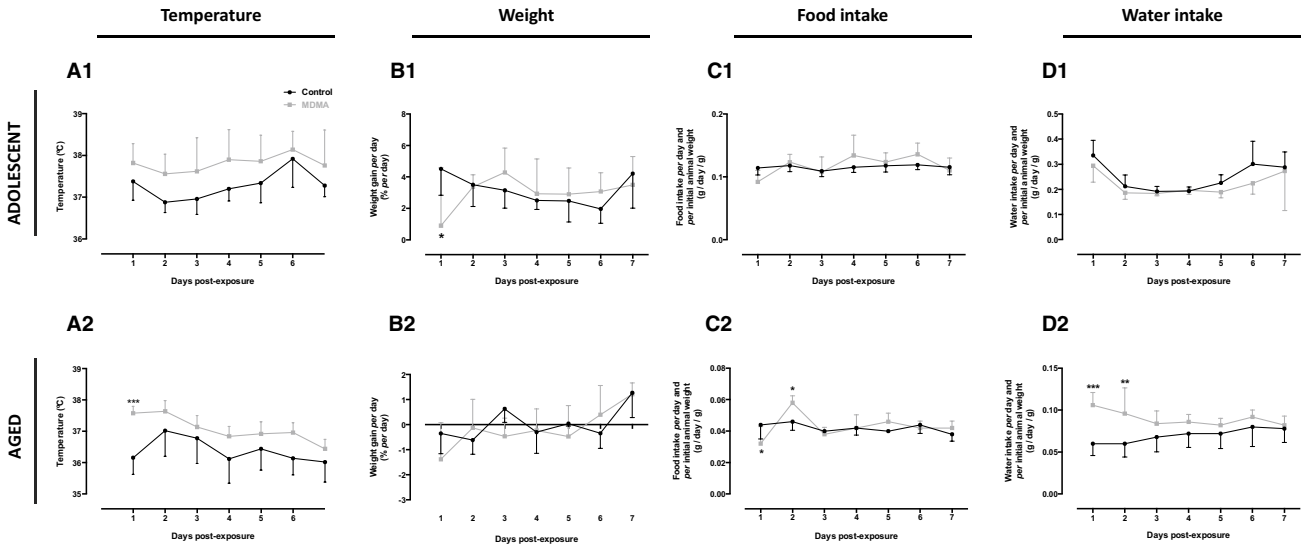

Fig. 2 Temperature, animal weight, food and water intake in adolescent [control $n=5$; MDMA $n=5$] and aged [control $n=5$; MDMA $n=5$] groups along the 7 days following "ecstasy" administration. (A) Temperature (°C) of the control and the MDMA groups, of either the adolescent (**A1**) or aged (**A2**) animals. (B) Weight gain *per* day (percentage of weight gain *per* day) post-treatment of the control and MDMA groups for the adolescent (**B1**) or aged (**B2**) animals. (C) Food intake *per* day and *per* initial weight (g/day/g), of the control and MDMA group, for the adolescent (**C1**) or aged (**C2**) animals. (D) Water intake *per* day and *per* initial weight (g/day/g), of the control and MDMA group, for the adolescent (**D1**) or aged (**D2**) animals (*$p<0.05$, **$p<0.01$ and ***$p<0.001$ MDMA versus control at the same timepoint)

Neurotoxicity- and brain-associated changes after MDMA exposure

MDMA promoted serotonergic neurotoxicity in aged, but not in adolescent rats

MDMA exposure has been associated with long-term depletion of brain serotonergic markers, an indicator of long-term neurotoxicity (Capela et al. 2009). 7 days after MDMA exposure, the levels of 5-HT in four brain areas, hippocampus, frontal cortex, striatum and cerebellum were assessed. In adolescent animals, the binge dose of MDMA (3×5 mg/kg) did not alter the 5-HT levels on the hippocampus (Fig. 3A1), the frontal cortex (Fig. 3A3), the striatum (Fig. 3A5) or on the cerebellum (Fig. 3A7), when comparing to respective control levels. When assessing 5-HT brain levels of aged animals, a significant decrease on the hippocampus of the MDMA-treated group (2×5 mg/kg) was observed (Fig. 3A2). No differences to controls were found on the 5-HT levels of the frontal cortex (Fig. 3A4), striatum (Fig. 3A6) or cerebellum (Fig. 3A8) of aged animals treated with MDMA. These results point for a higher susceptibility of aged animals, and in particular the hippocampus, in terms of serotonergic neurotoxicity of MDMA.

It was only possible to measure the levels of the 5-HT metabolite, 5-HIAA, (Fig. 3B) and DA (Fig. 3C) in the striatum. No significant differences in 5-HIAA or DA were found in the striatum of control and MDMA-treated rats in either adolescent (Fig. 3B1, C1) or aged (Fig. 3B2, C2) groups.

Noteworthy, differences among animal age in terms of brain tissue 5-HT levels were seen. In the hippocampus and striatum of adolescent rats, 5-HT levels were approximately the double of those found in aged animals (Fig. 3A1–2, A5–6). Regarding the 5-HT metabolite, the levels measured in the striatum of adolescent rats were approximately four times higher than those found in aged animals (Fig. 3B1–2). There were also remarkable differences in terms of DA content in the striatum, as adolescent animals showed *circa* four times higher levels than aged rats (Fig. 3C1–2).

MDMA evoked an increase in Tau protein phosphorylation in the brain of aged, but not adolescent rats

We examined whether MDMA evoked in rats an increase in brain tau protein phosphorylation (p-Tau). Considering the adolescent population, there were no differences between the MDMA and control groups in p-Tau Ser396 immunoreactivity across the four brain regions evaluated (Fig. 4A1, A3, A5, A7). However, in the aged group, a significant increase in Tau phosphorylation at Ser396 was observed in the hippocampus (Fig. 4A2), striatum (Fig. 4A6) and cerebellum (Fig. 4A8) of MDMA-treated animals. Meanwhile, in the frontal cortex of aged animals, the difference among control and MDMA-treated rats was not significant (Fig. 4A4).

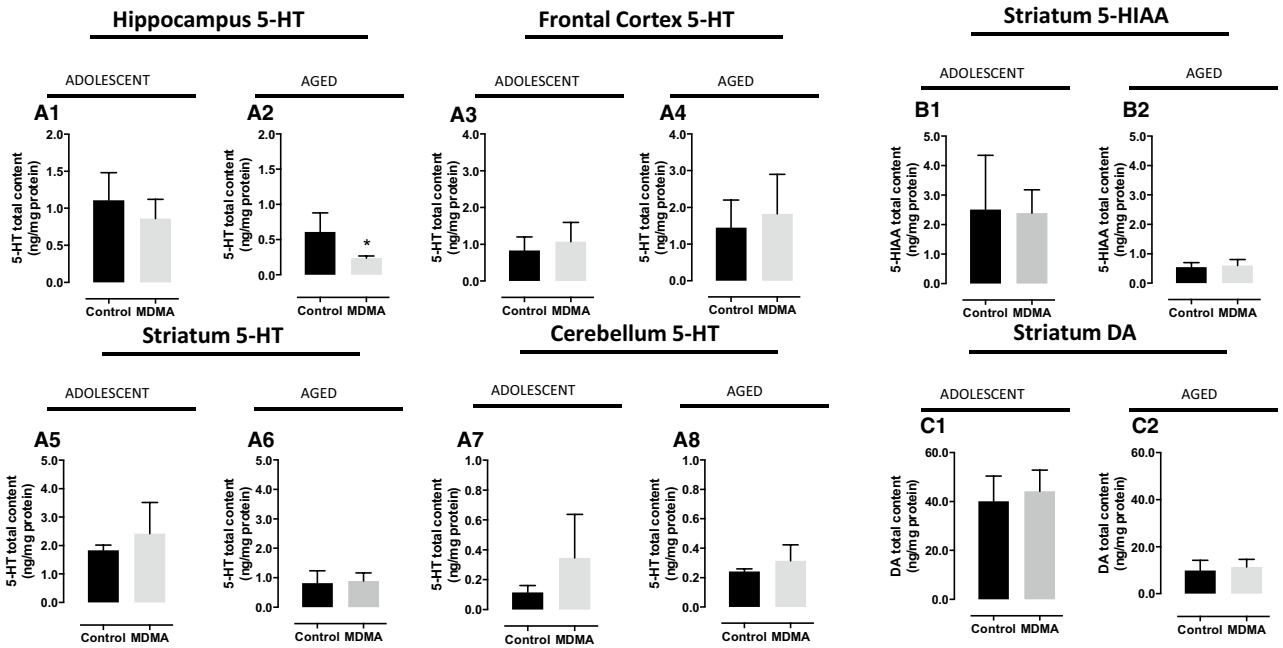

Fig. 3 Serotonin (5-HT) levels in the four brain areas, as well as 5-hydroxyindoleacetic acid (5-HIAA) and dopamine (DA) levels in the striatum of adolescent and aged animals. (A) Total content of 5-HT in the hippocampus for the adolescent [control $n=5$; MDMA $n=5$] (**A1**) and aged [control $=4$; MDMA $n=5$] (**A2**) groups; cortex for the adolescent [control $n=4$; MDMA $n=5$] (**A3**) and aged [control $n=4$; MDMA $n=5$] (**A4**) groups; striatum for the adolescent [control $n=4$; MDMA $n=5$] (**A5**) and the aged [control $n=4$; MDMA $n=4$] (**A6**) groups; and in the cerebellum for the adolescent [control $n=4$; MDMA $n=5$] (**A7**) and aged [control $n=4$; MDMA $n=5$] (**A8**) animals. (B) Total content of 5-HIAA in the striatum of the adolescent [control $n=5$; MDMA $n=5$] (**B1**) and the aged [control $n=4$; MDMA $n=4$] (**B2**) animals. (C) Total content of DA in the striatum of the adolescent [control $n=5$; MDMA $n=5$] (**C1**) and the aged [control $n=5$; MDMA $n=5$] (**C2**) animals ($^*p<0.05$ MDMA versus control)

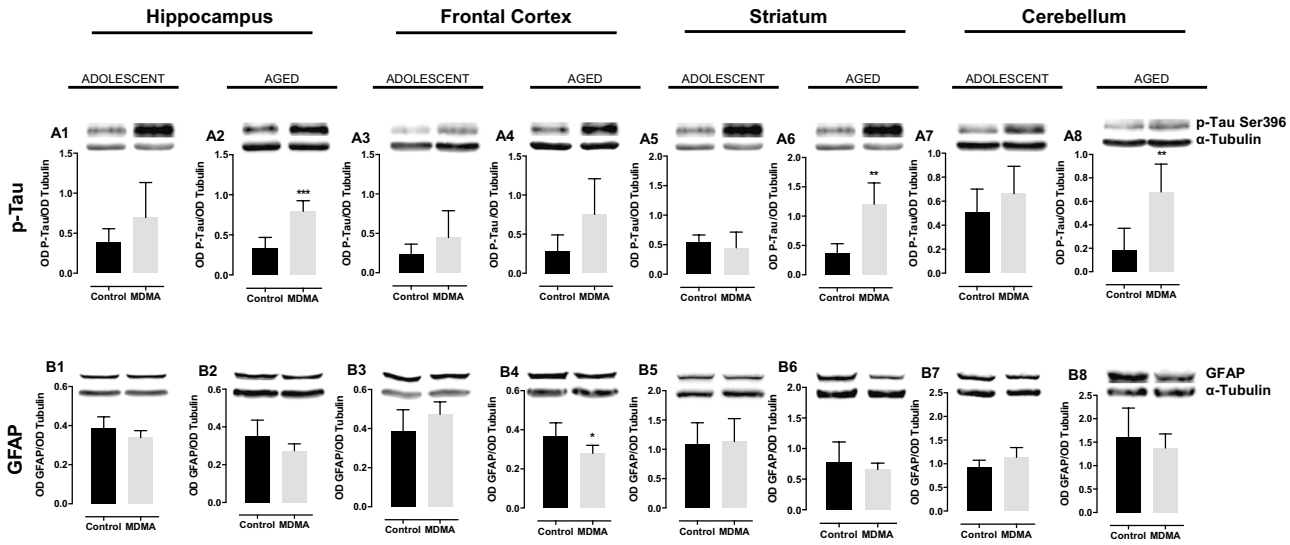

Fig. 4 Western blot analysis of phospho-tau Ser396 (p-Tau) and glial fibrillary acidic protein (GFAP) levels in the brain areas of adolescent [control $n=5$; MDMA $n=5$] and aged [control $n=5$; MDMA $n=5$] animals. (A) Optic density (OD) of p-Tau normalized to the OD of α-tubulin in the hippocampus of the adolescent (**A1**) and the aged (**A2**) animals; frontal cortex of the adolescent (**A3**) and the aged (**A4**) groups; striatum of the adolescent (**A5**) and the aged (**A6**) groups; cerebellum of the adolescent (**A7**) and the aged groups (**A8**). (B) Glial fibrillary acidic protein (GFAP) content normalized to the OD of α-tubulin in the hippocampus of the adolescent (**B1**) and the aged (**B2**) groups; in the frontal cortex of the adolescent (**B3**) and the aged (**B4**) groups; in the striatum of the adolescent (**B5**) and the aged (**B6**) groups; and in the cerebellum of the adolescent (**B7**) and the aged (**B8**) groups ($^*p<0.05$, $^{**}p<0.01$, $^{***}p<0.001$ MDMA versus control)

Reactive astrogliosis and increases in the brain levels of GFAP have been associated to several neurotoxic insults, though many times absent in the case of MDMA-induced neurotoxicity (Capela et al. 2009). The MDMA-treated adolescent animals showed no differences in GFAP expression in all four brain areas analyzed (Fig. 4B1, B3, B5, B7), when comparing to the controls. Meanwhile, in the frontal cortex of aged rats MDMA promoted a significant decrease in GFAP protein content, when compared to the control group (Fig. 4B4). In the hippocampus, striatum, or cerebellum of aged animals, no differences were found between the control and the MDMA-exposed group regarding the GFAP expression (Fig. 4B2, B6, B8).

MDMA-evoked brain oxidative stress in both adolescent and aged rats

The formation of reactive oxygen species has been shown to be involved in MDMA-mediated neurotoxic events (Capela et al. 2009; Teixeira-Gomes et al. 2016). Several biochemical markers related to oxidative stress were measured to ascertain its contribution for MDMA-evoked events 7 days after treatment. In the MDMA-treated adolescent animals, a significant increase in protein carbonylation was observed in the hippocampus, frontal cortex, and in the striatum (Fig. 5A1, A3, A5), while no differences were found in the cerebellum (Fig. 5A7). In aged animals, protein carbonylation increased in the hippocampus and striatum of MDMA-treated rats (Fig. 5A2, A6). As for the frontal cortex or cerebellum of aged rats, no differences in protein carbonylation were found between MDMA-treated and control animals (Fig. 5A4, A8).

The assessment of 4-HNE brain content did not reveal any increases following MDMA exposure in the four brain areas of both aged and adolescent animals (Fig. 5B). However, there was a significant decrease on the hippocampal 4-HNE content of MDMA-exposed aged rats (Fig. 5B2).

Another indicator of oxidative stress-related changes, quinoprotein levels, revealed a significant increase in the adolescent frontal cortex, when compared to the control animals (Fig. 5C3). Meanwhile, no differences were found in the other brain areas of adolescent rats (Fig. 5C1, C5, C7). On the aged group, no differences were found between control and MDMA-exposed animals in all brain areas analyzed (Fig. 5C2, C4, C6, C8).

The levels of GSH and the ratio of GSH/GSSG were also evaluated in the brain of MDMA-administered animals 7 days following treatment. Only in the hippocampus

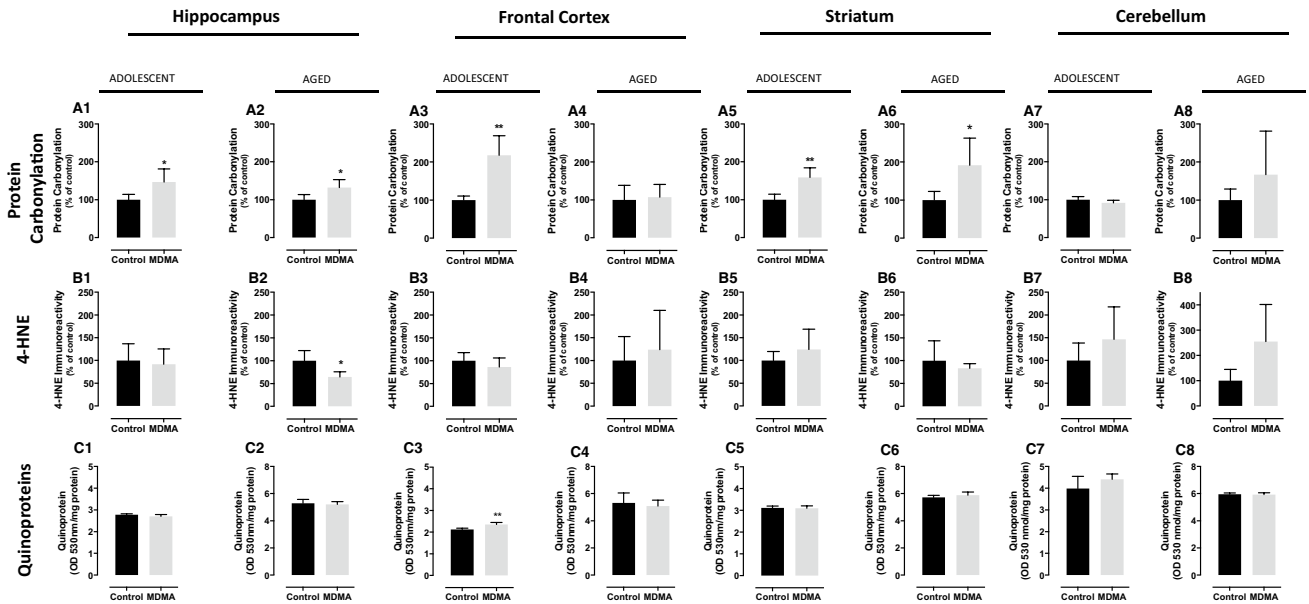

Fig. 5 Oxidative stress parameters in the brain areas of adolescent [control $n=5$; MDMA $n=5$] and aged [control $n=5$; MDMA $n=5$] animals exposed to MDMA. (A) Protein carbonylation levels expressed in percentage of controls in the hippocampus of adolescent (**A1**) and the aged (**A2**) animals; in the frontal cortex of the adolescent (**A3**) and the aged (**A4**) animals; the striatum of the adolescent (**A5**) and the aged (**A6**) animals; and in the cerebellum of the adolescent (**A7**) and the aged (**A8**) animals. (B) 4-Hydroxynonenal (4-HNE) levels expressed in percentage of controls in the hippocampus of the adolescent (**B1**) and the aged (**B2**) animals; in the frontal cortex of the adolescent (**B3**) and the aged (**B4**) animals; the striatum of the adolescent (**B5**) and the aged (**B6**) animals; and in the cerebellum of the adolescent (**B7**) and the aged (**B8**) animals. (**C**) Quinoproteins levels are presented as the OD 530 nm/mg of protein in the hippocampus of the adolescent (**C1**) and the aged (**C2**) animals; in the frontal cortex of the adolescent (**C3**) and the aged (**C4**) animals; in the striatum of the adolescent (**C5**) and the aged (**C6**) animals; and the cerebellum of the adolescent (**C7**) and the aged animals (**C8**) (*$p<0.05$, **$p<0.01$ MDMA versus control)

of aged animals, a significant decrease in total GSH levels was found, when compared to the controls (Table 1), and no significant differences were found on the GSH/GSSG ratio content in that same brain area. Of note, control-aged animals had about three times less total GSH in the hippocampus than control adolescents, meanwhile for other brain areas analyzed values were similar. Regarding the other brain regions, no differences were found in aged animals in both total GSH and GSH/GSSG ratios (Table 1). No changes were found in adolescent rats in terms of total GSH or GSH/GSSG ratio following MDMA exposure on all brain areas analyzed (Table 1).

The cerebellum of aged animals presented lower ATP levels following MDMA exposure

The brain energetic levels were also assessed in both populations. A significant decrease on ATP levels in the cerebellum of aged rats exposed to MDMA was found, when compared to controls (Table 1). No differences were found on the hippocampus, cortex or striatum of the aged group. Regarding the adolescent group, no differences were found between control and MDMA-treated animals across all brain areas studied (Table 1).

Peripheral organ-associated changes following MDMA exposure

MDMA promoted vascular congestion in the heart and kidneys of adolescent and aged animals: a higher susceptibility of the aged kidney

To evaluate the damage promoted by MDMA to the peripheral organs, we performed an histological observation of heart, kidney and liver tissue sections following routine hematoxylin/eosin staining. Histological evaluation of adolescent heart tissue from MDMA-treated rats showed several morphological differences, when compared to controls (Fig. 6A1). 7 days following exposure to MDMA, the heart of adolescent rats (Fig. 6A2) showed widespread vascular congestion, with enlarged blood vessels filled with abundant red blood cells (Fig. 6A2, A3). A general enlargement of intercellular space, suggestive of interstitial oedema, was also notorious (Fig. 6A3). No signals of intracellular oedema in cardiomyocytes were observed in these animals. When compared to controls (Fig. 6B1), the heart of MDMA-treated aged rats (Fig. 6B2) revealed intense vascular congestion and interstitial oedema. Moreover, some clusters of cardiomyocytes evidencing signs of intracellular oedema, suggested by the enlarged intermyofibrillar space and by the presence of a white perinuclear halo, were also observed (Fig. 6B3). Of note, the vascular congestion and the interstitial oedema seen in the heart tissue of MDMA-treated aged animals were more intense than those found in their adolescent counterparts.

Table 1 Total glutathione (total GSH), the ratio of reduced (GSH) and oxidized (GSSG) levels, and adenosine triphosphate (ATP) levels, in the hippocampus, frontal cortex, striatum, and cerebellum of adolescent [control $n=5$, MDMA $n=5$; exception for hippocampus GSH/GSSG control $n=5$, MDMA $n=4$] and aged [control $n=5$, MDMA $n=5$] groups 7 days after MDMA exposure

Parameter	Adolescents		Aged	
	Control	MDMA	Control	MDMA
Hippocampus				
Total GSH (nmol/mg protein)	48.80 ± 3.92	51.00 ± 6.28	16.72 ± 1.66	14.48 ± 0.66*
GSH/GSSG	72.06 ± 12.49	64.06 ± 10.48	41.81 ± 8.02	41.35 ± 1.90
ATP (nmol/mg protein)	5.46 ± 0.82	5.71 ± 1.46	2.11 ± 0.60	2.67 ± 0.72
Frontal cortex				
Total GSH (nmol/mg protein)	39.98 ± 4.81	45.96 ± 7.97	28.62 ± 5.24	26.50 ± 3.29
GSH/GSSG	69.60 ± 18.89	59.45 ± 5.94	36.69 ± 4.51	39.18 ± 6.32
ATP (nmol/mg protein)	14.70 ± 11.17	10.10 ± 3.19	2.84 ± 0.76	3.99 ± 1.28
Striatum				
Total GSH (nmol/mg protein)	12.39 ± 1.05	12.37 ± 1.53	13.20 ± 0.97	13.51 ± 0.79
GSH/GSSG	13.12 ± 2.11	10.87 ± 3.43	25.83 ± 6.17	29.93 ± 2.77
ATP (nmol/mg protein)	5.37 ± 0.89	6.58 ± 0.78	2.29 ± 0.56	2.45 ± 0.27
Cerebellum				
Total GSH (nmol/mg protein)	9.72 ± 1.04	9.83 ± 0.80	9.54 ± 1.15	9.45 ± 1.21
GSH/GSSG	14.02 ± 0.82	14.47 ± 3.02	16.18 ± 2.21	14.42 ± 1.52
ATP (nmol/mg protein)	1.97 ± 0.22	2.00 ± 0.42	3.01 ± 0.45	2.16 ± 0.42*

Results are expressed in nmol per mg of protein (nmol/mg protein) (*$p<0.05$ MDMA versus control)

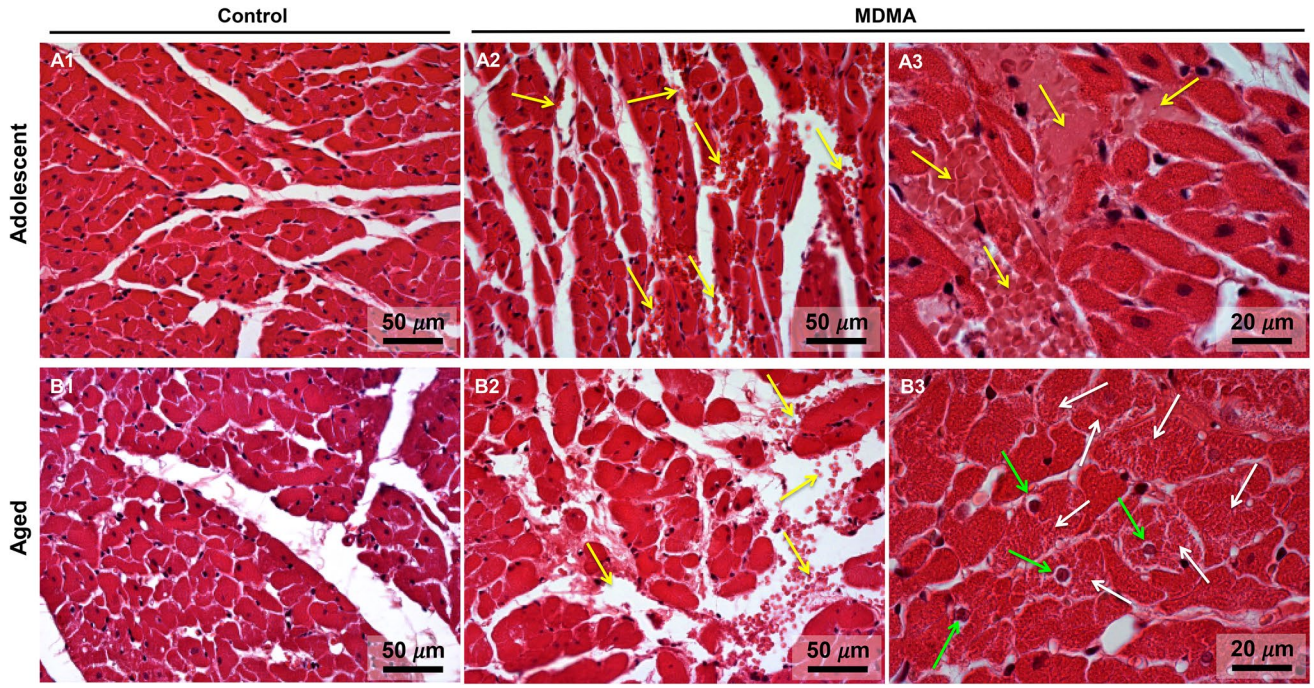

Fig. 6 Representative microphotographs of heart tissue from adolescent (**A1, A2**, and **A3**) and aged animals (**B1, B2**, and **B3**), stained with hematoxylin/eosin. The heart of adolescent and aged controls (**A1, B1**) showed a normal structure. In MDMA-exposed adolescent animals (**A2, A3**), it can be seen vascular congestion (yellow arrows), with abundant blood vessels filled with erythrocytes and fibrin-like material. In aged animals treated with MDMA, the vascular congestion is also marked (**B2**, yellow arrows), being depicted in **B3** a cluster of oedematous cardiomyocytes evidenced by the white perinuclear halo (green arrows) and by the enlargement of intermyofibrillar space (white arrows). The enlargement of interstitial space is notorious in **A2** and **B2**, being more pronounced in aged animals. (Color figure online)

When evaluating the kidney tissue of the adolescent group (Fig. 7A1–3), vascular congestion was present in MDMA-treated animals (Fig. 7A2), as suggested by the enlarged vessels and glomerular capillaries, with erythrocytes and deposition of fibrin-like material in the glomeruli and periglomerular capillaries (Fig. 7A3). Importantly, the kidneys of aged animals revealed the most dramatic changes (Fig. 7B1–3). The kidney tissue of MDMA-exposed aged animals showed an enlargement of the blood vessels with accumulation of erythrocytes in their interior, as well as proximal tubules with frequent oedematous/necrotic cells (Fig. 7B2). The glomeruli of aged animals exposed to MDMA, when compared to controls, presented an apparent atrophy with loss of endothelial cell nucleus, with enlargement of Bowman's space (Fig. 7B3). Apparently, the renal injury caused by MDMA to aged rats was higher when compared to adolescent animals, with special affectation of the glomeruli.

In sections stained with hematoxylin/eosin, the liver tissue of adolescent and aged animals showed no differences between the respective control and MDMA-treated groups (data not shown).

Several plasma biochemical parameters, which are generally regarded as biomarkers of heart and liver damage, were also assessed. 7 days post-MDMA exposure, no statistically significant changes in plasma levels of ALT, AST/ALT ratio, CKMB and CK-R were found in the MDMA-exposed animals (Table 2). Only the plasma levels of AST were significantly decreased in MDMA-exposed aged animals (Table 2).

MDMA promoted the increase of collagen/fibrotic tissue in the liver of both adolescent and aged animals

Sirius red staining was performed to evaluate the presence of fibrosis in the three peripheral organs analyzed. In the liver tissue, there was a significant increase on the collagen percentage in both adolescent and aged MDMA-treated rats when compared to their control counterparts (Table 3). Evaluation of the percentage of collagen present in the heart (Table 4) and kidney (Table 5) of adolescent or aged animals showed no differences between MDMA-treated and saline-treated animals.

Despite the above described tissue changes, caspase 3, 8 and 9 activities were not increased on the liver, heart or kidneys of either adolescent or aged animals 7 days following exposure to MDMA, when compared to their respective control groups (Tables 3, 4, 5). However, the activities of caspase 3 and 8 in the liver of MDMA-treated adolescent

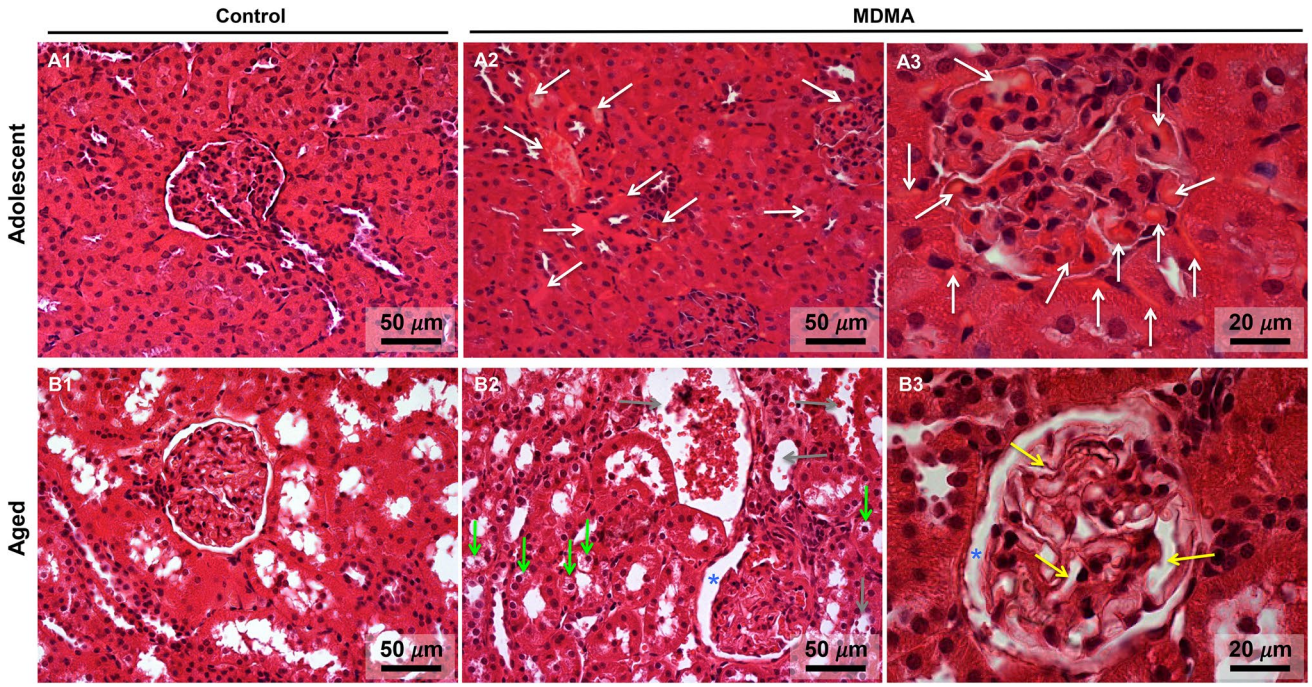

Fig. 7 Representative microphotographs of kidney tissue from adolescent (**A1, A2**, and **A3**) and aged animals (**B1, B2**, and **B3**), stained with hematoxylin/eosin. The kidney of adolescent and aged controls (**A1, B1**) showed a normal structure, with **B1** presenting a light enlargement of proximal tubules with cellular debris within, explained by an age effect paralleled with the used method of fixation by diffusion. In adolescent MDMA-treated animals (**A2, A3**), several blood vessels filled with erythrocytes and fibrin-like material, suggestive of vascular congestion (white arrows), are depicted in **A2**; in this group, capillary congestion, within the glomerulus and in periglomerular space, was also notorious (**A3**, white arrows). In aged animals exposed to MDMA (**B2, B3**), it can be observed in B2 several oedematous/necrotic cells in the proximal tubules (green arrows), signs of vascular congestion (grey arrows), and a glomerulus with enlarged Bowman's space (asterisk); in the other microphotograph from this group (**B3**), the dilation of glomerular capillaries with reduced number of endothelial nuclei (yellow arrows) and the enlargement of Bowman's space (asterisk) are also depicted. (Color figure online)

Table 2 Plasma biochemical parameters in the adolescent [AST and ALT, control $n=5$, MDMA $n=5$; CKMB, control $n=4$ and MDMA $n=5$; CK-R, control $n=4$, MDMA $n=4$] and aged [AST, CKMB, and CK-R, control $n=5$, MDMA $n=5$; ALT, control $n=5$, MDMA $n=4$] groups 7 days after MDMA exposure

Parameter	Adolescents		Aged	
	Control	MDMA	Control	MDMA
AST (U/L)	106.20 ± 34.82	73.80 ± 8.67	156.40 ± 89.71	49.20 ± 39.52*
ALT (U/L)	54.80 ± 9.42	43.00 ± 16.36	35.80 ± 7.79	26.00 ± 5.94
AST/ALT ratio	1.90 ± 0.37	2.04 ± 1.08	4.63 ± 2.79	2.60 ± 1.76
CKMB (U/L)	403.50 ± 327.29	315.40 ± 101.41	183.00 ± 35.02	165.00 ± 27.83
CK-R (U/L)	270.4 ± 171.58	164.60 ± 31.49	173.20 ± 19.58	146.00 ± 35.04

Results are expressed in units per liter (U/L) (*$p<0.05$ MDMA versus control)

rats were significantly lower than their respective controls (Table 3).

To exclude any difference in organ weight, we also evaluated the relative weight at the time of killing. There were no differences between the control and the MDMA-treated groups regarding the liver, heart or kidney weight *per* brain weight ratio (Tables 3, 4, 5) in both adolescent and aged groups.

No changes in oxidative stress and in ATP levels were evoked by MDMA in the peripheral organs

Several oxidative stress parameters were determined in the three peripheral organs. None of the studied parameters was significantly altered following exposure to MDMA, in either adolescent or aged populations. The total GSH levels and the GSH/GSSG ratio were not altered in the liver,

Table 3 Biochemical and histological parameters analyzed in the liver of adolescent [$n=5$, MDMA $n=5$; exception for caspase 3 and 8, control $n=5$, MDMA $n=4$; collagen ratio, control $n=3$, MDMA $n=3$] and aged [control $n=5$, MDMA $n=5$; exception for collagen ratio, control $n=3$, MDMA $n=3$] groups 7 days after MDMA exposure

Parameter	Adolescents		Aged	
	Control	MDMA	Control	MDMA
Liver weight/brain weight ratio	5.00 ± 0.49	4.80 ± 0.63	8.21 ± 0.90	7.33 ± 0.93
Total GSH (nmol/mg protein)	70.22 ± 8.10	58.48 ± 18.59	35.80 ± 4.92	31.29 ± 7.50
GSH/GSSG	34.33 ± 6.16	32.01 ± 12.84	19.75 ± 6.53	18.07 ± 5.09
Quinoproteins (OD530nm/mg protein)	4.15 ± 0.25	4.41 ± 0.60	6.09 ± 0.24	5.91 ± 0.38
Protein carbonylation (%control)	100.00 ± 18.57	93.55 ± 12.28	100.00 ± 15.95	99.76 ± 27.11
ATP (nmol/mg protein)	0.76 ± 0.35	0.76 ± 0.29	0.48 ± 0.27	0.59 ± 0.30
Caspase 3 activity (FU/μg protein)	3.78 ± 0.95	2.44 ± 0.21*	0.60 ± 0.27	0.83 ± 0.36
Caspase 9 activity (FU/μg protein)	2.62 ± 0.54	2.06 ± 0.72	0.53 ± 0.21	0.72 ± 0.24
Caspase 8 activity (FU/μg protein)	2.67 ± 0.54	1.75 ± 0.16*	0.38 ± 0.16	0.48 ± 0.11
Collagen ratio (% collagen/cells)	0.03 ± 0.02	0.05 ± 0.02*	0.04 ± 0.03	0.07 ± 0.04*

*$p < 0.05$ MDMA versus control

Table 4 Biochemical and histological parameters analyzed in the heart of adolescent [$n=5$, MDMA $n=5$; exception for collagen ratio, control $n=3$, MDMA $n=3$] and aged [control $n=5$, MDMA $n=5$; exception for ATP, control $n=4$, MDMA $n=5$; collagen ratio, control $n=3$, MDMA $n=3$] groups 7 days after MDMA exposure

Parameter	Adolescents		Aged	
	Control	MDMA	Control	MDMA
Heart weight/brain weight ratio	0.40 ± 0.03	0.40 ± 0.06	0.67 ± 0.08	0.64 ± 0.05
Total GSH (nmol/mg protein)	13.01 ± 2.49	13.56 ± 1.48	6.99 ± 1.84	7.22 ± 1.77
GSH/GSSG (nmol/mg protein)	8.21 ± 3.39	6.67 ± 2.23	12.44 ± 6.88	11.64 ± 6.77
Quinoproteins (OD530nm/mg protein)	8.56 ± 0.72	8.15 ± 0.52	5.31 ± 0.44	5.32 ± 0.20
Protein carbonylation (%control)	100.00 ± 34.64	100.75 ± 43.17	100.00 ± 19.55	87.40 ± 10.64
ATP (nmol/mg protein)	0.80 ± 0.25	0.86 ± 0.21	0.29 ± 0.07	0.71 ± 0.59
Caspase 3 activity (FU/μg protein)	1.51 ± 0.26	1.45 ± 0.37	0.22 ± 0.09	0.24 ± 0.12
Caspase 9 activity (FU/μg protein)	0.98 ± 0.30	0.98 ± 0.50	0.18 ± 0.09	0.20 ± 0.13
Caspase 8 activity (FU/μg protein)	2.50 ± 0.47	2.26 ± 0.42	0.36 ± 0.08	0.37 ± 0.17
Collagen ratio (% collagen/cells)	0.05 ± 0.04	0.03 ± 0.02	0.04 ± 0.04	0.04 ± 0.03

Table 5 Biochemical and histological parameters analyzed in the kidney of adolescent [$n=5$, MDMA $n=5$; exception for total GSH, control $n=5$, MDMA $n=4$; collagen ratio, control $n=3$, MDMA $n=3$] and aged [control $n=5$, MDMA $n=5$; exception for caspase 3, control $n=5$, MDMA $n=4$; collagen ratio, control $n=3$, MDMA $n=3$] groups 7 days after MDMA exposure

Parameter	Adolescents		Aged	
	Control	MDMA	Control	MDMA
Kidneys weight/brain weight ratio	0.93 ± 0.05	0.87 ± 0.13	1.59 ± 0.21	1.38 ± 0.15
Total GSH (nmol/mg protein)	2.97 ± 0.57	3.31 ± 0.04	2.52 ± 0.50	4.14 ± 1.97
GSH/GSSG (nmol/mg protein)	55.31 ± 12.88	52.79 ± 15.09	79.86 ± 65.76	50.01 ± 20.62
Quinoproteins (OD530nm/mg protein)	6.56 ± 1.44	7.18 ± 1.14	4.81 ± 0.43	4.90 ± 1.53
Protein carbonylation (%control)	100.00 ± 15.31	101.67 ± 8.98	100.00 ± 15.95	96.76 ± 27.11
ATP (nmol/mg protein)	0.72 ± 0.31	0.93 ± 0.23	0.29 ± 0.21	0.71 ± 0.59
Caspase 3 activity (FU/μg protein)	2.30 ± 0.65	2.44 ± 0.63	0.72 ± 0.15	0.70 ± 0.08
Caspase 9 activity (FU/μg protein)	2.79 ± 0.75	3.20 ± 0.54	0.79 ± 0.20	1.03 ± 0.25
Caspase 8 activity (FU/μg protein)	2.12 ± 0.70	2.21 ± 0.22	0.54 ± 0.13	0.65 ± 0.15
Collagen ratio (% collagen/cells)	0.12 ± 0.07	0.10 ± 0.07	0.08 ± 0.03	0.07 ± 0.04

heart or kidneys in either group following MDMA treatment (Tables 3, 4, 5). In agreement with these results, no differences were found in quinoprotein levels or protein carbonylation across all organs and animal groups (Tables 3, 4, 5). It is also interesting to note the great differences seen among animal age in terms of total GSH. The cardiac and hepatic levels of total GSH in adolescent rats were roughly the double of those found on aged animals.

When assessing the ATP levels in the three organs, no significant differences were found between the control and MDMA-treated groups in either adolescent or aged rats (Tables 3, 4, 5).

Discussion

The present work revealed the differential toxic effects of MDMA in adolescent and aged rats, using MDMA doses comparable to human "ecstasy" intake. This study was the first to use aged rats to evaluate the effects of MDMA. Our major findings were: (1) aged animals are more prone to MDMA-evoked hyperthermia than adolescents; (2) MDMA-induced serotonergic neurotoxicity in the hippocampus of aged animals, but not in any brain area of adolescent rats; (3) MDMA promoted an increase in Tau phosphorylation, a biochemical hallmark of several neurodegenerative disorders, again only in the brain of aged animals; (4) MDMA evoked brain protein carbonylation in the hippocampus and striatum of aged animals and in the hippocampus, frontal cortex, and striatum brain areas of adolescent animals, but only decreased total GSH levels in the hippocampus of MDMA-treated aged animals; (5) Aged animals were more susceptible to MDMA-mediated histological damage in the heart and kidneys, than their adolescent counterparts; (6) MDMA treatment promoted an increase in liver fibrotic tissue both in aged and in adolescent animals.

Many reports have shown the acute hyperthermic effects of MDMA to rats [for a review see (Capela et al. 2009)]. However, only a few research groups have explored the role of aging in MDMA-induced hyperthermia. Aged rats presented a more robust hyperthermia than adolescents (maximal temperature increase of 3 °C versus 1 °C), and aged animals showed thermoregulatory impairment revealing signs of hyperthermia on the next day post-exposure. The differential susceptibility of adolescents versus aged animals to MDMA evoked hyperthermia may be a contributing factor for other differences found following drug exposure. Previous studies in rats and mice conducted with adolescent and young adult animals have also shown a distinct hyperthermic response following MDMA, but no study, to the best of our knowledge, has explored the aged rats' response. In male Sprague–Dawley rats and using higher MDMA doses (20 and 40 mg/kg, given orally) than our study, it was found that a single MDMA dose could elicit a more robust hyperthermic response in PND 70 than in PND 40 rats (Broening et al. 1995). In addition, 10-week-old C57Bl/6J mice presented a higher magnitude of response than 4-week-old counterparts, after exposure to (+)-MDMA (20 mg/kg × 4, s.c.) (Reveron et al. 2005). Thus, older animals seem more prone to present a more robust hyperthermic response to MDMA.

In our study, aged animals were the only group that showed differences in terms of water and food intake during the next 2 days after MDMA exposure. The high temperatures reached by these animals in the day of exposure, followed by the thermoregulation impairment strongly contributed to these effects in aged animals, which were not seen in their younger counterparts. No changes in body weight were verified in both ages 7 days following MDMA exposure, despite the known anorectic effect of amphetamines (Teixeira-Gomes et al. 2015). We previously reported no differences among control and MDMA-treated adolescent PND40 rats regarding body weight gain, food, or water intake, 24 h after exposure to the same dose scheme used in adolescent animals in the present study (Teixeira-Gomes et al. 2016). Therefore, MDMA evoked changes to the brain and peripheral organs are unlikely related to changes in body-weight, water and food intake.

MDMA neurotoxicity is generally accompanied by a long-term decrease in serotonergic markers, including depletion of 5-HT and its main metabolite 5-HIAA, as well as SERT and TPH immunoreactivity (Alves et al. 2009; Capela et al. 2009; Colado et al. 1997; Goni-Allo et al. 2008a; Teixeira-Gomes et al. 2015). We proved that aged animals are more susceptible to MDMA-induced serotonergic neurotoxicity than adolescent rats. In fact, aged MDMA-treated rats were the only group that revealed 5-HT depletion in the hippocampus 7 days following exposure. The MDMA dose regimen used in the adolescent group (3 × 5 mg/kg, every 2 h, i.p.) was previously proven in adult male Wistar rats to promote serotonergic neurotoxicity, leading to a decrease in the 5-HT levels and its metabolite 5-HIAA in the hippocampus, frontal cortex and striatum (Goni-Allo et al. 2008a). Therefore, there are important and consistent differences among adolescent, adult and aged rats in terms of vulnerability to the serotonergic neurotoxicity promoted by MDMA, and the hippocampus is clearly more vulnerable. In fact, susceptibility of the serotonergic system is markedly increased when exposure to MDMA occurs in adulthood (Teixeira-Gomes et al. 2015).

A correlation between hyperthermia and serotonergic neurotoxicity has been clearly established (Malberg and Seiden 1998). In adult rats, increases in core animal temperature potentiated MDMA-induced serotonergic neurotoxicity (Goni-Allo et al. 2008a; Malberg and Seiden 1998). However, many drugs that protect against MDMA-induced neurotoxicity do not interfere with the hyperthermic response evoked by MDMA, such as fluoxetine (Malberg et al. 1996) or selegiline (Alves et al. 2007), ruling that hyperthermia is not crucial for MDMA-evoked serotonergic neurotoxicity. Additionally, body temperature can interfere with MDMA metabolism. The administration of MDMA (3 × 5 mg/kg, every 2 h, i.p.) to adult rats at a 30 °C environmental temperature leaded to an increase in plasma concentrations of MDMA metabolites, 6 h after the first MDMA injection, when compared to rats at 15 and 21 °C (Goni-Allo et al. 2008a). It might therefore be assumed that the higher core body temperature found in aged rats might be an

important explanation for the potentiation of serotonergic neurotoxicity.

The stage of brain development and the maturity of metabolic pathways are important factors when exploring the differences among adults, adolescents and aged animals. On the other hand, MDMA metabolites are known to be neurotoxic and play an important role in MDMA neurotoxic events (Barbosa et al. 2014a, b; Capela et al. 2006, 2007, 2009). There might be important differences among ages in terms of MDMA metabolism, although this remains to be clarified. In addition, the maturational stage of the 5-HT projections might be relevant. In fact, a previous study found that reductions in SERT binding were less pronounced in several brain areas of adolescent rats when compared to adult rats (PND38 in adolescent animals and PND74 in adult animals at the time of analysis) 7 days after MDMA exposure of male Wistar rats (10 mg/kg, subcutaneous, b.i.d, 4 days) (Klomp et al. 2012). In our study, only the hippocampus of aged rats revealed 5-HT depletion promoted by MDMA, meanwhile other brain areas were not affected. The hippocampus is known to be strongly affected by MDMA-mediated long-lasting neurotoxicity (Capela et al. 2009). A recent study analyzed the recovery of serotonergic fibers in Dark Agouti rats, following exposure to a single neurotoxic dose of MDMA (15 mg/kg, i.p.) (Ádori et al. 2011). These researchers found that 6 months after exposure only the hippocampus presented decreased TPH immunoreactivity, meanwhile in the cortex and caudate putamen there was an earlier recovery (Ádori et al. 2011). It is known that the hippocampus is highly enervated by serotonergic fibers, but a decreased serotonergic innervation of the hippocampal formation is known to occur during aging (Nishimura et al. 1995; van Luijtelaar et al. 1988). As we showed, control aged animals revealed lower levels of 5-HT in the hippocampus than their adolescent counterparts, rendering them more prone to neurotoxic actions. Overall, aging seems to play a role in MDMA serotonergic neurotoxicity. Of note, the depletion of 5-HT in the hippocampus of aged animals was not accompanied by an increase in GFAP immunoreactivity, which is in accordance to other studies (Capela et al. 2009). Using the same dose scheme of our study, a recent report also showed the absence of GFAP activation in male Sprague–Dawley rats aged PND 33 or PND 54, 24 h following exposure during 1 day or during 4 days of MDMA (3 × 5 mg/kg, i.p., every 2 h) (Garcia-Cabrerizo and Garcia-Fuster 2015). Also, in agreement, Ádori and co-workers reported no differences in the hippocampus, cortex, and caudate putamen brain areas regarding the GFAP astroglia marker and the isolectin B4 microglia marker in 24–25-month-old rats, which were treated with MDMA at adolescent/young adult age with an intermittent regimen (15 mg/kg, i.p., every 7th day for 4 weeks) or with a single-dose regimen (15 mg/kg, i.p.) (Ádori et al. 2011).

Enhanced Tau phosphorylation is a hallmark of Alzheimer's disease and other chronic neurodegenerative diseases, and Tau hyperphosphorylation causes instability in the microtubules leading to neurodegeneration (Iqbal et al. 2009). Only aged rats revealed an increase in Tau Ser396 phosphorylation in the hippocampus, striatum and cerebellum, 7 days following exposure to MDMA, ruling for a long-lasting event not seen in MDMA-treated adolescent animals. The wide range of brain areas affected proves that the MDMA-prompted instability to the microtubules is not restricted to a single brain area. A previous study conducted in 10-week-old C57BL/6 mice exposed 6 days to high MDMA doses [cumulative doses of 60 or 180 mg/kg (10 or 30 mg/kg, daily for 6 days, i.p.)] revealed increased p-Tau levels in the CA2/CA3 regions of the hippocampus 1 week after treatment (Busceti et al. 2008). These events argue for robust brain changes associated to MDMA misuse that go beyond serotonergic neurotoxicity. The combination of 5-HT depletion, oxidative stress, and Tau Ser396 phosphorylation in the hippocampus directs for a higher susceptibility of this brain area to MDMA neurotoxic actions. Aging and MDMA may cooperate for the development of neurological disorders linked to p-Tau. Moreover, the hippocampus vulnerability to MDMA neurotoxic actions raises the possibility of specific neurological disorders linked to this brain area, given its important role in memory and learning.

Oxidative stress-related changes have been reported in the brain of animals exposed to MDMA and other amphetamines, and several contributing factors for MDMA-induced oxidative stress have been raised, including the formation of redox-active MDMA metabolites, monoamine neurotransmitters metabolism by monoamine oxidase, nitric oxide formation and hyperthermia (Barbosa et al. 2012, 2014b; Capela et al. 2009; Carvalho et al. 2012; Teixeira-Gomes et al. 2015). In our paradigm of exposure, MDMA evoked brain oxidative stress in both adolescent and aged rats, as evaluated by several parameters. However, only the hippocampus of aged animals showed lower levels of total GSH, while no changes were seen in other areas. The lack of changes in the brain GSH levels of adolescent rats is in agreement with our previous results obtained 24 h after exposure to MDMA in adolescents (Teixeira-Gomes et al. 2016). In fact, the hippocampus of control aged animals had a total GSH content about three times lower than their adolescent counterparts, which certainly renders aged animals more susceptible to oxidative stress. We can speculate that brain oxidative stress-related changes develop over time and become evident days following MDMA exposure. Thus, the hippocampus is once more a critical area affected by MDMA-evoked oxidative stress.

Amphetamines are known to interfere with ATP levels, promote neuronal mitochondrial dysfunction and impair mitochondrial neuronal trafficking (Barbosa et al. 2014c,

2015). MDMA only decreased ATP levels in the cerebellum of aged animals, while other brain areas were not affected. We previously reported that MDMA induced a decrease in ATP levels in the frontal cortex of male adolescent PND40 Wistar rats, 24 h after exposure to the dose scheme used herein (Teixeira-Gomes et al. 2016). Therefore, we can conclude that in adolescent animals, ATP decreases in the frontal cortex are not long-lasting and a recovery occurs, unlike aged animals where changes in the cerebellum were not transient. The cerebellum brain area is known to possess low SERT levels, and most studies either conduced in humans (Klomp et al. 2012) or in animals (Ádori et al. 2011; Goni-Allo et al. 2008a; Malberg and Seiden 1998) do not evaluate this brain area following MDMA exposure. In fact, the cerebellum is generally used as a reference for background radioactivity in neuroimaging studies that evaluate SERT density (Klomp et al. 2012). However, bilateral gray matter concentration reductions in the cerebellar hemispheres were found in a study conducted with MDMA polydrug users using a voxel-based morphometry technique (Cowan et al. 2003). The decrease in ATP levels coupled to the increase in Tau phosphorylation seen in the cerebellum of aged animals point out the vulnerability of this brain area to MDMA toxicity.

Human reports of heart, renal and liver injuries in MDMA users have been well documented and are a great challenge to professionals in intensive care units (Greene et al. 2003; Hall and Henry 2006). We report that aged animals were more prone to MDMA-induced renal and cardiac tissue damage when compared to adolescent animals. Although aged animals, *per se*, revealed lower levels of GSH in the peripheral organs (cardiac and hepatic levels of total GSH were about two times lower) in comparison to their adolescent counterparts, the aged population did not show a higher susceptibility in terms of oxidative damage following MDMA exposure.

The vascular changes and structural damage observed in the heart and kidneys of either adolescent or aged animals, 7 days after exposure to MDMA, are suggestive of prolonged organ tissue disturbances. Two important factors can be postulated as determinants for these events: the MDMA-evoked hyperthermia and the cardiovascular response. Previously, we have shown that MDMA promoted significant histological tissue alterations, including vascular congestion, in the liver, heart and kidneys of PND40 adolescent Wistar rats, 24 h after the same MDMA dose regimen used herein (3 × 5 mg/kg, every 2 h, i.p.) (Teixeira-Gomes et al. 2016). It was reported that Wistar rats exposed for 30 min to temperatures of 40.5 °C present vascular stasis and enlarged blood vessels in the heart and kidneys (Vlad et al. 2010). Consistent with the major role of hyperthermia is the fact that tissue damage was more severe in aged animals, which developed a remarkable hyperthermia that was still present on the next day following MDMA exposure. Previous reports conducted in laboratory animals have confirmed the ability of MDMA to produce serious cardiac toxicity. In rats either single MDMA doses (20 mg/kg, i.p.) (Shintani-ishida et al. 2014) or MDMA binges (four cycles of MDMA dosing, each consisting of 9 mg/kg, b.i.d., i.v for 4 days, separated by a 10 day drug-free period) (Shenouda et al. 2008) were shown to produce left ventricular dysfunction. In rats, disrupted cytoarchitecture and necrosis were observed in the hearts of adult animals treated with a high cumulative MDMA dose, three binge administrations of MDMA (each binge of 9 mg/kg intravenous, b.i.d., for 4 days) (Badon et al. 2002). The hearts of adolescent male Sprague–Dawley rats (7-week-old) 24 h after a single MDMA dose (20 mg/kg, i.p.) presented autophagic vacuoles in the cardiomyocytes seen by electron microscopy (Shintani-ishida et al. 2014). MDMA activated the autophagy-lysosomal pathway and the released lysosomal proteases damage myofibrils that may lead to left ventricular systolic dysfunction and altered cytoarchitecture in rat heart (Shintani-ishida et al. 2014). The literature on the renal histopathologic observations after MDMA is very scarce. We found a single study reporting necrosis, haemorrhage and oedema in the kidneys of male albino mice weighing 25–30 g following 24 h exposure to MDMA (20 mg/ kg, i.p.) (Karami et al. 2014). Our study not only illustrates the differential susceptibility of ages towards MDMA heart and kidney toxicity, but also highlights that tissue damage in peripheral organs might be long-lasting.

MDMA is a known sympathomimetic drug that promotes the release of NA not only in the brain but also in the peripheral organs (Capela et al. 2009; Teixeira-Gomes et al. 2015). A recent study evaluated the cardiac sympathetic activity and the cellular stress in adolescent naive male CD-1 mice that were killed 48 h (PND 40), 72 h (PND 41) or 7 days (PND 45) after MDMA administration (20 mg/kg × 2, i.p.) (Navarro-Zaragoza et al. 2015). In the left ventricle of MDMA-treated mice, the NA and normetanephrine content increased, as well as the normetanephrine / NA ratio 72 h after MDMA exposure, while TH phosphorylation at serine 31, was increased 72 h and 7 days after MDMA, indicating an increased NA turnover and sympathetic cardiac activity (Navarro-Zaragoza et al. 2015). In parallel with the described modifications in the cardiac sympathetic activity, an increase in HSP27 expression (72 h) and phosphorylation (7 days) was seen in the left ventricle following MDMA exposure, supporting the idea that it exacerbates cellular stress (Navarro-Zaragoza et al. 2015). Thus, it seems reasonable that the observed cardiac damage is partially dependent on MDMA-increased sympathetic tone.

Caspases form an intracellular proteolytic cascade during apoptosis, and have an important role in apoptotic events during development, tissue remodeling, cell homeostasis, defense processes and immune responses (Bantel et al.

2001). Despite the changes verified in the tissues of the three peripheral organs following MDMA exposure, we did not find an increase in caspase activity in any MDMA-treated group. In accordance, our previous study in adolescent rats did not show an increase in caspase 3, 8 or 9 activities in the liver, heart or kidneys 24 h following exposure to MDMA (Teixeira-Gomes et al. 2016). Altogether, apoptosis does not seem to be involved either in the short or in the long-term effects of MDMA to the tissues. We could though speculate that the loss of cells seen in the kidney of aged animals treated with MDMA might involve necrosis. Interestingly, the liver of MDMA-treated adolescent animals showed a decline in the activity of caspase 3 and 8. In agreement, our previous study conducted with adolescent animals revealed lower caspase 8 activity in the liver of MDMA-treated animals 24 h post-exposure (Teixeira-Gomes et al. 2016). This decrease might be more related to a lower tissue remodeling, since hepatobiliary diseases are generally characterized by elevated caspase activation and apoptosis (Bantel et al. 2001). Despite the distinct effects in several parameters, both adolescent and aged animals developed an increase in the liver fibrotic tissue after MDMA exposure, while they did not show any signs of liver damage in the haematoxylin/eosin histological examination. It is known that chronic liver inflammation may lead to fibrosis and cirrhosis (Szabo and Csak 2012). We did not find any signs of increased levels of immune cells in the liver and we did not evaluate markers of inflammation, but we can speculate that an inflammatory process may have preceded the liver fibrosis. MDMA liver metabolism is known to produce highly reactive metabolites (Capela et al. 2009), which associated with hyperthermia may be the cause for the increase in the fibrotic tissue seen in the liver of MDMA-treated animals. Juvenile male CD-1 mice treated with mitoxantrone showed an increase in cardiac fibrotic tissue, accompanied by a decrease in caspase 3 activity (Dores-Sousa et al. 2015). Therefore, the increase in fibrotic tissue that we saw in the liver of MDMA treated rats can be accompanied by a decrease in caspase 3 activity, since that increase may not be linked to apoptosis.

The heart and kidneys are known to receive considerable sympathetic enervation and are subjected to high catecholamine levels (Costa et al. 2011; de Champlain et al. 1967) and they showed marked histological damage following MDMA, while the liver with low catecholamine content (de Champlain et al. 1967) did not reveal any vascular changes. Altogether, these results point out to the importance of increased sympathetic activity and the release of NA in MDMA-induced adverse events to peripheral organs. In fact, the body temperature increase following "ecstasy" may result from the activation of the sympathetic nervous system and the hypothalamic–pituitary–thyroid/adrenal axis (Mills et al. 2004). Our age distinct effects might also be due to differences among ages to the heat stressor. In line with our results, in senescent rats, altered NA turnover was reported during heating (Kregel 1994). Fischer 344 rats heated to 41.0 °C demonstrated marked elevations in NA turnover in the left ventricle, renal cortex, liver, and adrenal gland, which was significantly higher in the kidney and liver of senescent (24 months old) rats compared to their mature (12 months old) counterparts (Kregel 1994). Therefore, MDMA evoked hyperthermia and increased sympathetic activity may cooperate together to evoke a more robust damage in the heart and kidney tissue of aged animals.

In summary, there are important age differences in the toxic events promoted by "ecstasy" in relevant doses to the human scenario of drug usage. The hippocampus of aged animals revealed 5-HT neurotoxicity following MDMA, while no neurotransmitter changes were seen in their adolescent counterparts. In addition, aged animals are more susceptible than adolescent rats to tissue damage in the heart and kidneys following "ecstasy", thus suggesting a direct relationship between the age of the "ecstasy" user and MDMA-related toxic events.

Acknowledgements We greatly acknowledge Dr. ª Bárbara Oliveira of ICBAS-UP animal house facility, and Dr.ª Laura Pereira of FFUP biochemistry for their technical assistance. This work was supported by the Fundação para a Ciência e Tecnologia (FCT)—Project PTDC/SAU-FCF/102958/2008—QREN initiative with EU/FEDER financing through under the frame of ''Programa Operacional Temático Factores de Competitividade (COMPETE) do Quadro Comunitário de Apoio III'' and ''Fundo Comunitário Europeu (FEDER)'' (FCOMP-01-0124-FEDER-011079). It was also supported by FEDER funds through the COMPETE and by national funds by the Fundação para a Ciência e Tecnologia (FCT) within the Project "PTDC/DTP-FTO/1489/2014—POCI-01-0145-FEDER-016537". This work also received financial support from the European Union (FEDER funds POCI/01/0145/FEDER/007728) and National Funds (FCT/MEC, Fundação para a Ciência e a Tecnologia and Ministério da Educação e Ciência) under the Partnership Agreement PT2020 UID/MULTI/04378/2013. Additionally, supported by project NORTE-01-0145-FEDER-000024, supported by Norte Portugal Regional Operational Programme (NORTE 2020), under the PORTUGAL 2020 Partnership Agreement (DESignBIOtecHealth—New Technologies for three Health Challenges of Modern Societies: Diabetes, Drug Abuse and Kidney Diseases), through the European Regional Development Fund (ERDF). VM Costa and DJ Barbosa acknowledge FCT for their post-doc (SFRH/BPD/110001/2015) and PhD grants (SFRH/BD/64939/2009), respectively.

Compliance with ethical standards

Conflict of interest The authors declare that they have no conflict of interest.

Disclosure Parts of this work have been presented orally at the Portuguese Pharmacology Society annual meeting, and in the form of an abstract and poster at the Congress of the European Societies of Toxicology (Eurotox). Some results included in this article were incorporated in Armanda Gomes Master thesis entitled "Brain and Peripheral Organ Toxicity of "Ecstasy" in Adolescent Rats in Human Relevant Doses" printed last September 2014. The thesis document is available online at the university of Porto repository: https://repositorio-aberto.up.pt/bitstream/10216/76843/2/32960.pdf.

References

Ádori C, Andó RD, Szekeres M, Gutknecht L, Kovács GG, Hunyady L, Lesch K-P, Bagdy G (2011) Recovery and aging of serotonergic fibers after single and intermittent MDMA treatment in dark agouti rat. J Comp Neurol 519(12):2353–2378. https://doi.org/10.1002/cne.22631

Alves E, Summavielle T, Alves CJ, Gomes-da-Silva J, Barata JC, Fernandes E, Bastos ML, Tavares MA, Carvalho F (2007) Monoamine oxidase-B mediates ecstasy-induced neurotoxic effects to adolescent rat brain mitochondria. J Neurosci 27(38):10203–10210. https://doi.org/10.1523/jneurosci.2645-07.2007

Alves E, Binienda Z, Carvalho F, Alves CJ, Fernandes E, Bastos ML, Tavares MA, Summavielle T (2009) Acetyl-l-carnitine provides effective in vivo neuroprotection over 3,4-methylenedioximethamphetamine-induced mitochondrial neurotoxicity in the adolescent rat brain. Neuroscience 158(2):514–523. https://doi.org/10.1016/j.neuroscience.2008.10.041

Andreu V, Mas A, Bruguera M, Salmeron JM, Moreno V, Nogue S, Rodes J (1998) Ecstasy: a common cause of severe acute hepatotoxicity. J Hepatol 29(3):394–397. https://doi.org/10.1016/S0168-8278(98)80056-1

Armenian P, Mamantov TM, Tsutaoka BT, Gerona RR, Silman EF, Wu AH, Olson KR (2013) Multiple MDMA (Ecstasy) overdoses at a rave event: a case series. J Intensive Care Med 28(4):252–258. https://doi.org/10.1177/0885066612445982

Badon LA, Hicks A, Lord K, Ogden BA, Meleg-Smith S, Varner KJ (2002) Changes in cardiovascular responsiveness and cardiotoxicity elicited during binge administration of Ecstasy. J Pharmacol Exp Ther 302(3):898–907. https://doi.org/10.1124/jpet.302.3.898

Bantel H, Ruck P, Gregor M, Schulze-Osthoff K (2001) Detection of elevated caspase activation and early apoptosis in liver diseases. Eur J Cell Biol 80(3):230–239. https://doi.org/10.1078/0171-9335-00154

Barbosa DJ, Capela JP, Oliveira JM, Silva R, Ferreira LM, Siopa F, Branco PS, Fernandes E, Duarte JA, Bastos ML, Carvalho F (2012) Pro-oxidant effects of Ecstasy and its metabolites in mouse brain synaptosomes. Br J Pharmacol 165(4b):1017–1033. https://doi.org/10.1111/j.1476-5381.2011.01453.x

Barbosa DJ, Capela JP, Silva R, Vilas-Boas V, Ferreira LM, Branco PS, Fernandes E, Bastos ML, Carvalho F (2014a) The mixture of "ecstasy" and its metabolites is toxic to human SH-SY5Y differentiated cells at in vivo relevant concentrations. Arch Toxicol 88(2):455–473. https://doi.org/10.1007/s00204-013-1120-7

Barbosa DJ, Serrat R, Mirra S, Quevedo M, de Barreda EG, Avila J, Ferreira LM, Branco PS, Fernandes E, Bastos ML, Capela JP, Soriano E, Carvalho F (2014b) The mixture of "ecstasy" and its metabolites impairs mitochondrial fusion/fission equilibrium and trafficking in hippocampal neurons, at in vivo relevant concentrations. Toxicol Sci 139(2):407–420. https://doi.org/10.1093/toxsci/kfu042

Barbosa DJ, Serrat R, Mirra S, Quevedo M, Gómez de Barreda E, Ávila J, Fernandes E, Bastos ML, Capela JP, Carvalho F, Soriano E (2014c) MDMA impairs mitochondrial neuronal trafficking in a Tau- and Mitofusin2/Drp1-dependent manner. Arch Toxicol 88(8):1561–1572. https://doi.org/10.1007/s00204-014-1209-7

Barbosa DJ, Capela JP, Feio-Azevedo R, Teixeira-Gomes A, Bastos ML, Carvalho F (2015) Mitochondria: key players in the neurotoxic effects of amphetamines. Arch Toxicol 89(10):1695–1725. https://doi.org/10.1007/s00204-015-1478-9

Beck BD, Seeley M, Calabrese EJ (2014) The use of toxicology in the regulatory process. In: Wallace Hayes A, Kruger CL (eds) Haye's principles and methods of toxicology, 6th edn. CRC Press, Boca Raton, pp 35–87

Broening HW, Bowyer JF, Slikker W (1995) Age-dependent sensitivity of rats to the long-term effects of the serotonergic neurotoxicant (+/−)-3,4-methylenedioxymethamphetamine (MDMA) correlates with the magnitude of the MDMA-induced thermal response. J Pharmacol Exp Ther 275(1):325–333

Busceti CL, Biagioni F, Riozzi B, Battaglia G, Storto M, Cinque C, Molinaro G, Gradini R, Caricasole A, Canudas AM, Bruno V, Nicoletti F, Fornai F (2008) Enhanced tau phosphorylation in the Hippocampus of Mice Treated with 3,4-methylenedioxymethamphetamine ("Ecstasy"). J Neurosci 28(12):3234–3245. https://doi.org/10.1523/jneurosci.0159-08.2008

Capela JP, Meisel A, Abreu AR, Branco PS, Ferreira LM, Lobo AM, Remiao F, Bastos ML, Carvalho F (2006) Neurotoxicity of Ecstasy metabolites in rat cortical neurons, and influence of hyperthermia. J Pharmacol Exp Ther 316(1):53–61. https://doi.org/10.1124/jpet.105.092577

Capela JP, Macedo C, Branco PS, Ferreira LM, Lobo AM, Fernandes E, Remiao F, Bastos ML, Dirnagl U, Meisel A, Carvalho F (2007) Neurotoxicity mechanisms of thioether ecstasy metabolites. Neuroscience 146(4):1743–1757. https://doi.org/10.1016/j.neuroscience.2007.03.028

Capela JP, Carmo H, Remiao F, Bastos ML, Meisel A, Carvalho F (2009) Molecular and cellular mechanisms of ecstasy-induced neurotoxicity: an overview. Mol Neurobiol 39(3):210–271. https://doi.org/10.1007/s12035-009-8064-1

Carvalho M, Carmo H, Costa VM, Capela JP, Pontes H, Remião F, Carvalho F, Bastos ML (2012) Toxicity of amphetamines: an update. Arch Toxicol 86(8):1167–1231. https://doi.org/10.1007/s00204-012-0815-5

Che S, Johnson M, Hanson GR, Gibb JW (1995) Body temperature effect on methylenedioxymethamphetamine-induced acute decrease in tryptophan hydroxylase activity. Eur J Pharmacol 293(4):447–453

Colado MI, O'Shea E, Granados R, Misra A, Murray TK, Green AR (1997) A study of the neurotoxic effect of MDMA ('ecstasy') on 5-HT neurones in the brains of mothers and neonates following administration of the drug during pregnancy. Br J Pharmacol 121(4):827–833. https://doi.org/10.1038/sj.bjp.0701201

Costa VM, Silva R, Ferreira LM, Branco PS, Carvalho F, Bastos ML, Carvalho RA, Carvalho M, Remiao F (2007) Oxidation process of adrenaline in freshly isolated rat cardiomyocytes: formation of adrenochrome, quinoproteins, and GSH adduct. Chem Res Toxicol 20(8):1183–1191. https://doi.org/10.1021/tx7000916

Costa VM, Carvalho F, Bastos ML, Carvalho RA, Carvalho M, Remiao F (2011) Contribution of catecholamine reactive intermediates and oxidative stress to the pathologic features of heart diseases. Curr Med Chem 18(15):2272–2314. https://doi.org/10.2174/092986711795656081

Cowan RL, Lyoo IK, Sung SM, Ahn KH, Kim MJ, Hwang J, Haga E, Vimal RLP, Lukas SE, Renshaw PF (2003) Reduced cortical gray matter density in human MDMA (Ecstasy) users: a voxel-based morphometry study. Drug Alcohol Depend 72(3):225–235. https://doi.org/10.1016/j.drugalcdep.2003.07.001

Cuyas E, Robledo P, Pizarro N, Farre M, Puerta E, Aguirre N, de la Torre R (2014) 3,4-methylenedioxymethamphetamine induces gene expression changes in rats related to serotonergic and dopaminergic systems, but not to neurotoxicity. Neurotox Res 25(2):161–169. https://doi.org/10.1007/s12640-013-9416-1

de Champlain J, Krakoff LR, Axelrod J (1967) Catecholamine Metabolism in Experimental Hypertension in the Rat. Circ Res 20(1):136–145. https://doi.org/10.1161/01.res.20.1.136

Dores-Sousa JL, Duarte JA, Seabra V, Bastos ML, Carvalho F, Costa VM (2015) The age factor for mitoxantrone's cardiotoxicity: Multiple doses render the adult mouse heart more susceptible to injury. Toxicology 329:106–119. https://doi.org/10.1016/j.tox.2015.01.006

EMCDDA (2017) European Drug Report 2017: Trends and developments. European Monitoring Centre for Drugs and Drug Addiction, Luxembourg

Garcia-Cabrerizo R, Garcia-Fuster MJ (2015) Chronic MDMA induces neurochemical changes in the hippocampus of adolescent and young adult rats: down-regulation of apoptotic markers. Neurotoxicology 49:104–113. https://doi.org/10.1016/j.neuro.2015.06.001

Goni-Allo B, Mathuna BO, Segura M, Puerta E, Lasheras B, de la Torre R, Aguirre N (2008a) The relationship between core body temperature and 3,4-methylenedioxymethamphetamine metabolism in rats: implications for neurotoxicity. Psychopharmacology 197(2):263–278. https://doi.org/10.1007/s00213-007-1027-1

Goni-Allo B, Puerta E, Mathuna BO, Hervias I, Lasheras B, de la Torre R, Aguirre N (2008b) On the role of tyrosine and peripheral metabolism in 3,4-methylenedioxymethamphetamine-induced serotonin neurotoxicity in rats. Neuropharmacology 54(5):885–900. https://doi.org/10.1016/j.neuropharm.2008.01.007

Greene SL, Dargan PI, O'Connor N, Jones AL, Kerins M (2003) Multiple toxicity from 3,4-methylenedioxymethamphetamine ("ecstasy"). Am J Emerg Med 21(2):121–124. https://doi.org/10.1053/ajem.2003.50028

Hall AP, Henry JA (2006) Acute toxic effects of 'Ecstasy' (MDMA) and related compounds: overview of pathophysiology and clinical management. Br J Anaesth 96(6):678–685. https://doi.org/10.1093/bja/ael078

Henry JA, Jeffreys KJ, Dawling S (1992) Toxicity and deaths from 3,4-methylenedioxymethamphetamine ("ecstasy"). Lancet 340(8816):384–387. https://doi.org/10.1016/0140-6736(92)91469-O

Iqbal K, Liu F, Gong C-X, Alonso AdC, Grundke-Iqbal I (2009) Mechanisms of tau-induced neurodegeneration. Acta Neuropathol 118(1):53–69. https://doi.org/10.1007/s00401-009-0486-3

Karami M, Karimian Nokabadi F, Ebrahimzadeh MA, Naghshvar F (2014) Nephroprotective effects of *Feijoa sellowiana* leaves extract on renal injury induced by acute dose of ecstasy (MDMA) in mice. Iran J Basic Med Sci 17(1):69–72

Kelly PA, Ritchie IM, Quate L, McBean DE, Olverman HJ (2002) Functional consequences of perinatal exposure to 3,4-methylenedioxymethamphetamine in rat brain. Br J Pharmacol 137(7):963–970. https://doi.org/10.1038/sj.bjp.0704961

Kindlundh-Hogberg AM, Schioth HB, Svenningsson P (2007) Repeated intermittent MDMA binges reduce DAT density in mice and SERT density in rats in reward regions of the adolescent brain. Neurotoxicology 28(6):1158–1169. https://doi.org/10.1016/j.neuro.2007.07.002

Klomp A, den Hollander B, de Bruin K, Booij J, Reneman L (2012) The effects of ecstasy (MDMA) on brain serotonin transporters are dependent on age-of-first exposure in recreational users and animals. PLoS One 7(10):e47524. https://doi.org/10.1371/journal.pone.0047524

Kolyaduke OV, Hughes RN (2013) Increased anxiety-related behavior in male and female adult rats following early and late adolescent exposure to 3,4-methylenedioxymethamphetamine (MDMA). Pharmacol Biochem Behav 103(4):742–749. https://doi.org/10.1016/j.pbb.2012.12.004

Kregel KC (1994) Influence of aging on tissue-specific noradrenergic activity at rest and during nonexertional heating in rats. J Appl Physiol 76(3):1226–1231. https://doi.org/10.1152/jappl.1994.76.3.1226

Loureiro-Vieira S, Costa VM, Duarte JA, Duarte-Araújo M, Gonçalves-Monteiro S, Bastos ML, Carvalho F, Capela JP (2018) Methylphenidate clinically oral doses improved brain and heart glutathione redox status and evoked renal and cardiac tissue injury in rats. Biomed Pharmacother 100:551–563. https://doi.org/10.1016/j.biopha.2018.02.017

Malberg JE, Seiden LS (1998) Small changes in ambient temperature cause large changes in 3,4-methylenedioxymethamphetamine (MDMA)-induced serotonin neurotoxicity and core body temperature in the rat. J Neurosci 18(13):5086–5094

Malberg JE, Sabol KE, Seiden LS (1996) Co-administration of MDMA with drugs that protect against MDMA neurotoxicity produces different effects on body temperature in the rat. J Pharmacol Exp Ther 278(1):258–267

Mills EM, Rusyniak DE, Sprague JE (2004) The role of the sympathetic nervous system and uncoupling proteins in the thermogenesis induced by 3,4-methylenedioxymethamphetamine. J Mol Med (Berl) 82(12):787–799. https://doi.org/10.1007/s00109-004-0591-7

Navarro-Zaragoza J, Ros-Simo C, Milanes MV, Valverde O, Laorden ML (2015) Binge ethanol and MDMA combination exacerbates toxic cardiac effects by inducing cellular stress. PLoS One 10(10):e0141502. https://doi.org/10.1371/journal.pone.0141502

Nishimura A, Ueda S, Takeuchi Y, Sawada T, Kawata M (1995) Age-related decrease of serotonergic fibres and S-100[beta] immunoreactivity in the rat dentate gyrus. Neuro Rep 6(10):1445–1448

Pereira FC, Gough B, Macedo TR, Ribeiro CF, Ali SF, Binienda ZK (2011) Buprenorphine modulates methamphetamine-induced dopamine dynamics in the rat caudate nucleus. Neurotox Res 19(1):94–101. https://doi.org/10.1007/s12640-009-9143-9

Reveron ME, Monks TJ, Duvauchelle CL (2005) Age-dependent (+)MDMA-mediated neurotoxicity in mice. Neurotoxicology 26(6):1031–1040. https://doi.org/10.1016/j.neuro.2005.05.006

Shenouda SK, Lord KC, McIlwain E, Lucchesi PA, Varner KJ (2008) Ecstasy produces left ventricular dysfunction and oxidative stress in rats. Cardiovasc Res 79(4):662–670. https://doi.org/10.1093/cvr/cvn129

Shintani-ishida K, Saka K, Yamaguchi K, Hayashida M, Nagai H, Takemura G, Yoshida K (2014) MDMA induces cardiac contractile dysfunction through autophagy upregulation and lysosome destabilization in rats. Biochim Biophys Acta 1842(5):691–700. https://doi.org/10.1016/j.bbadis.2014.01.013

Slotkin TA, Seidler FJ, Ali SF (2000) Cellular determinants of reduced adaptability of the aging brain: neurotransmitter utilization and cell signaling responses after MDMA lesions. Brain Res 879(1):163–173. https://doi.org/10.1016/S0006-8993(00)02767-0

Szabo G, Csak T (2012) Inflammasomes in liver diseases. J Hepatol 57(3):642–654. https://doi.org/10.1016/j.jhep.2012.03.035

Teixeira-Gomes A, Costa VM, Feio-Azevedo R, Bastos ML, Carvalho F, Capela JP (2015) The neurotoxicity of amphetamines during the adolescent period. Int J Dev Neurosci 41:44–62. https://doi.org/10.1016/j.ijdevneu.2014.12.001

Teixeira-Gomes A, Costa VM, Feio-Azevedo R, Duarte JA, Duarte-Araújo M, Fernandes E, Bastos ML, Carvalho F, Capela JP (2016) "Ecstasy" toxicity to adolescent rats following an acute low binge dose. BMC Pharmacol Toxicol 17(1):1–14. https://doi.org/10.1186/s40360-016-0070-0

UNODC (2017) World Drug Report 2017. United Nations, Vienna

van Luijtelaar MGPA, Steinbusch HWM, Tonnaer JADM (1988) Aberrant morphology of serotonergic fibers in the forebrain of the aged rat. Neurosci Lett 95(1–3):93–96. https://doi.org/10.1016/0304-3940(88)90638-6

Vlad M, Ionescu N, Ispas AT, Giuvarasteanu I, Ungureanu E, Stoica C (2010) Morphological changes during acute experimental short-term hyperthermia. Rom J Morphol Embryol 51(4):739–744

Yin C, Pettigrew A, Loftus JP, Black SJ, Belknap JK (2009) Tissue concentrations of 4-HNE in the black walnut extract model of laminitis: indication of oxidant stress in affected laminae. Vet Immunol Immunopathol 129(3–4):211–215. https://doi.org/10.1016/j.vetimm.2008.11.016